Les Cahiers du GERAD ISSN: 0711–2440

A stochastic optimisation model for the water pump scheduling problem with demand response in large and high altitude water supply systems

D. Cariaga, M. F. Anjos, Á. Lorca

G–2025–23

February 2025

La publication de ces rapports de recherche est rendue possible grâce au soutien de HEC Montréal, Polytechnique Montréal, Université McGill, Université du Québec à Montréal, ainsi que du Fonds de recherche du Québec – Nature et technologies.

Dépôt légal – Bibliothèque et Archives nationales du Québec, 2025
– Bibliothèque et Archives Canada, 2025

The publication of these research reports is made possible thanks to the support of HEC Montréal, Polytechnique Montréal, McGill University, Université du Québec à Montréal, as well as the Fonds de recherche du Québec – Nature et technologies.

Legal deposit – Bibliothèque et Archives nationales du Québec, 2025
– Library and Archives Canada, 2025

GERAD HEC Montréal
3000, chemin de la Côte-Sainte-Catherine
Montréal (Québec) Canada H3T 2A7

Tél. : 514 340-6053
Téléc. : 514 340-5665
info@gerad.ca
www.gerad.ca

A stochastic optimisation model for the water pump scheduling problem with demand response in large and high altitude water supply systems

Denise Cariaga [a, b, c]

Miguel F. Anjos [a, e]

Álvaro Lorca [b, c, d]

[a] *School of Mathematics, University of Edinburgh, Edinburgh, EH9 3FD, Scotland, UK*

[b] *Department of Industrial and Systems Engineering, Pontificia Universidad Católica de Chile, Santiago, 7820436, Chile*

[c] *UC Energy Research Centre, Pontificia Universidad Católica de Chile, Santiago, 7820436, Chile*

[d] *ECS-Lab at Department of Electrical Engineering, Pontificia Universidad Católica de Chile, Santiago, 7820436, Chile*

[e] *GERAD, Polytechnique Montreal, Montréal (Qc), Canada, H3T 1J4*

miguel.f.anjos@ed.ac.uk

February 2025
Les Cahiers du GERAD
G–2025–23

Abstract : The water pump scheduling problem is an optimisation model that determines which water pumps will be turned on or off at each time period over a given time horizon for a given water supply system. Water networks, as energy-intensive infrastructures, are promising candidates to offer the power system a reduction in their energy consumption during certain hours of the day; this service is known as demand response. The reduction is typically made during hours when there is a positive difference between the electricity spot price and the contracted energy price. However, both the spot price and the water demand are uncertain. Consequently, the pump scheduling problem with demand response faces several challenges from i) the non-linearities of the equations for the frictional losses along the pipes and pumps, which make the problem a nonlinear mixed-integer model, ii) the uncertainty from energy prices and water demand. These limitations prevent the problem from being solved to optimality in a reasonable computational time in water systems with more than two pumps and reservoirs. Therefore, we developed a new two-step stochastic optimisation model for the demand response in large and high-altitude water supply systems that uses a binary expansion approach to efficiently account for the existing nonlinearities by reducing the computational difficulties while maintaining an excellent representation of the physical phenomena involved. The first step uses a robust water profile optimisation model, and the second step uses a stochastic model for the power profile optimisation with a demand response to obtain the optimum water pump and demand response bidding schedule. We tested this approach using a case study from a mining company's water supply system. Our findings concluded that different seasons and energy policies, such as the minimum power requirement and availability bonus, can significantly impact the water supply system's total costs and the amount of demand response offered to the power system on the capacity market. Additionally, we included a proposal for energy policymakers to create the best strategies for demand response for water supply systems depending on the season of the year and energy prices in order to promote demand response provision on the water supply system operator side.

Keywords : Demand response, operation of water supply systems, flexible operation, nonlinear optimisation, water in mining

---

Acknowledgements: The authors thank ANID for their funding through the "DOCTORADO NACIONAL 21211385" scholarship, and CODELCO for their funding through the "Beneficio Piensa Minería". **Data Availability Statement:** Data available within the article or its supplementary materials. **Disclosure of interest:** No interests to declare.

1 Introduction

The optimal operation of water and energy networks is a relevant problem worldwide: the pumping system of a water network represents nearly 20% of the world's energy used by electric motors and 25–50% of the total electrical energy required in some industries [1], like e.g. in the Chilean mining due to its particular high altitude location in the Andes mountains. To add another layer of complexity, the operation of water networks can be affected due to changes in the availability of natural resources or due to public policies introduced in each country, such as restricting the use of spring water. Additionally, the increase in electrical demand has grown sharply in the last few years, mainly due to the development and expansion of new electricity usages: heat pumps, electric vehicles, and trains, among others [2]. Moreover, many countries committed to achieving carbon neutrality by 2050 in the 2015 Paris Agreement for Climate Action, which means carbon-fuelled energies will be replaced by renewable energies in the short-term [3]. However, renewable energies compromise the continuity and resilience of the electrical system due to weather uncertainty, so planning has become a key element in preventing shortages. Also, climate change has produced droughts in regions where it used to rain more frequently, weakening the water supply for hydropower, crops, industry, and human consumption, such as in the northern and central area in Chile [4].

With the Paris Energy Agreement, Chile has committed to achieve carbon neutrality by 2050 and the definitive closure of thermal power plants by 2040, closing 50% by 2025 [5]. By 2022, 62% of the installed capacity was renewable and 55,6% of the electricity generated in 2022 came from renewable energies [6]. At the beginning of 2022, the Chilean government announced their energy planning strategy, and they expect to achieve an 80% renewable mix by 2030, and a 100% by 2050 [7]. Having high penetration of renewable sources challenges the resilience of the electrical system due to climate variability. To embrace this variability, energy flexibility comes as a solution and is a requirement to ensure the resilience of the power system.

Energy flexibility is understood as the ability of a power system to respond to a change in load and generation. Also, it is said that a power system is flexible if it can, within economic boundaries, respond quickly to high fluctuations in supply and demand, ramping down a generation when demand decreases and upwards when it increases for scheduled and unpredictable events[8, 9]. Cochran et al. [10] distinguish four types of flexibility: generation, transmission, operation, and demand. In this project, we will focus on demand flexibility, which is provided by the demand side of a power system. Some common examples of demand flexibility devices are air conditioners, refrigerators, and heaters, as these may be shut down during stressful periods for the power system thus relieving it from generating electricity from non-renewable sources. However, these devices' energy consumption is not big enough to make a change in the energy demand. Therefore, they need an intermediate entity that links the small-demand clients with the power system, called an aggregator. Flexibility is ensured through ancillary services, which are the services necessary to support the transmission of electric power from generators to consumers.

A specific type of demand flexibility is the Demand Response (DR), and it is defined as the adaptation in electric usage by end-use customers from their standard consumption patterns in response to changes in the price of electricity over time, or it can also be defined as the incentive payments designed to induce lower electricity use at times of high wholesale market prices or when system reliability is jeopardised [11]. Price-based programs and Incentive-based programs are two ways to provide DR to the grid; the first one offers time-varying rates that reflect the value and cost of electricity in different periods, while the second pays participating customers to reduce their loads at times requested by the program sponsor. For both cases, the goal is to use electricity at lower prices or when the contract specifies to reduce consumption respectively.

The U S Department of Energy [11] states that the most important benefit of DR is improved resource-efficiency of electricity production due to closer alignment between customers' electricity prices and the value they place on electricity. Also, [12] argues that the environmental benefits of DR include better land utilisation as a result of avoided/deferred new electricity infrastructure, a quality improvement in air and water as a result of efficient use of resources, and a reduction of natural resources depletion. These benefits represent a crucial point for a faster renewable energy integration process to the grid. Some examples of recent works consider desalination plants [13–15], water heater aggregators [16, 17], water networks [2, 18–20], air conditioners [21, 22], and a mix of both [23].

Following the previous ideas, a promising alternative to provide demand flexibility –through ancillary services– to the electrical system are the water supply systems (WSSs) due to their high energy consumption [19, 24] and the water storage, which provides the flexible pumping. We found inspiration in Chilean mining through its WSS, which supplies desalinated water to each mining site. Nowadays, this industry faces a severe drought [25, 26], and the location of the mining operations accentuates this phenomenon since they are typically found at high altitudes, between 600 and 4000 meters above sea level [27]. The high altitude characteristic makes the operational model harder to solve due to the multiple combinations of pressure and water flow it has to compute [3]. In addition, due to legal and environmental restrictions that protect aquifers and national reserves, the option of extracting continental water is being increasingly reduced. In 2022, 34% of the water used in the copper mining industry came from the sea [28], and it is expected that by 2030 this will increase to 71% [29]. Thus, according to [30], the desalinated water pump would be the second most electricity-intensive process in copper mining, from 7% of the total in 2022 with 1.7 TWh to 15% with 4.7 TWh in 2033.

The DR model for WSS is an extension of the water pump scheduling problem which determines the optimal pump schedule to reduce operational costs. This problem is hard to solve due to its Non-Deterministic Polynomial-Time Hard (NP-Hard) nature [31], leading to high computational times, mainly due to i) the nonlinearities of the energy loss equations along pipes and pumps and the power used by pumps and ii) many possible combinations of head pressure and flow [32, 33]. There have been several research efforts on optimising the WSS operation models: heuristic optimisation methods with Dynamic Programming [34–36], hierarchical control methods [37–40], linear programming (LP) [41, 42], mixed-integer programming (MILP) with the Binary Expansion Approach [3], and nonlinear programming (NLP) [43]. A comprehensive review regarding WDS operational optimisation problems and solution methodologies is presented in [32, 44, 45].

The DR model for WSSs normally includes variable electricity prices or water demand uncertainty which some authors have treated in a stochastic or deterministic way. A branch and bound method is developed for the optimal pump scheduling problem in [18] which improves the energy efficiency of WSSs by shifting electricity consumption to low-price periods. Oikonomou et al. [19] created a two-step frequency regulation model for a WSS in California in coordination with the state's electrical system. Stuhlmacher and Mathieu [46] used a chance-constrained optimisation model for the water pumping problem connected to the power system. Mkireb et al. [2] developed a robust optimisation model for demand response power bids in the day-ahead market for drinking water networks in France. In [47], they proposed a deterministic optimisation framework for DR in a WSS, assuming the electricity price and the time when the DR is provided. Also, some works related to desalination plants have proposed demand response models using deterministic information of water and power demand forecasts [48], probabilistic models for weather in a small water and power network in the Canary Islands [14], and a simplified model for the day-ahead scheduling problem of power and desalination plants [13]. To summarise, even though these works integrated either the water demand uncertainty or the spot prices uncertainties, some of them assumed a known water pump scheduling and DR scheduling vector or didn't provide insights on how the power system could help the WSS operators reduce their costs more while providing the maximum DR possible, by ensuring the optimal energy policies.

Under this context, a challenge arises from analysing the ancillary services that the water pump scheduling problem can offer to the power system through its optimal bidding strategy, as a centralised WSS operator participating in the capacity market. All while minimising the WSS operational costs, and from studying the synergy between the energy and water system to propose future energy policies for the benefit of both systems. Therefore, the main goal of this paper is to develop an optimisation model for the water operations of WSS and energy networks to find optimal strategies to reduce systemic costs, promote renewable energy integration, and ensure the reliability and resilience of both water and energy networks, while accounting for the uncertainties coming from the water demand and electricity prices.

In this work, the main contributions are summarised as follows:

1. We optimised the water pump scheduling problem by offering demand response to the power system of high altitude WSS with multiple pumps and reservoirs using a discretised hourly time horizon with uncertain water demand and electricity spot prices. This model minimises the WSS total operational costs while delivering DR to the power system without compromising the water supply. The aim is to determine the optimal demand response bid on the capacity market from the point of view of the WSS operator, assuming that there is no payment for availability.
2. We proposed a two-step stochastic model for the water pump scheduling problem with demand response. The first step solves the water profile optimisation with a robust water demand. The second step calculates the power profile optimisation with demand response using stochastic spot prices. Finally, a validation model verifies the feasibility of the two-step model using simulated electricity prices.
3. We analysed the WSS of a mining company in Chile as a study case and studied different scenarios for the seasons of the year, water demand values, energy prices, and initial water level in tanks for each season of the year. The WSS utilised has an elevation of over 3000 meters, five water tanks, one reservoir and five water pumps. Our results show the effectiveness of the proposed approach in solving the problem and that providing demand response reduces the total operational costs for the WSS operator in all seasons and scenarios while ensuring the DR provision. Finally, we propose strategies to support energy policymakers in integrating demand response by WSS based on seasonal variations and electricity prices. The aim is to develop tools that incentivise WSS operators to participate in the capacity market as flexibility providers.

The remainder of this paper is organised as follows. In Section 2, we explain the proposed framework of the two-step stochastic model. In Section 3, we introduce the robust WSS operational model with uncertain water demand that delivers the optimal water profile. In Section 4, we define the stochastic demand response model for WSSs, including the uncertain spot prices response, which determines the optimal power profile. In Section 5, we propose two models to efficiently solve the water and power profile models. In Section 6, we evaluate the performance of the models using the real case of a WSS from a Chilean copper mining company and analysing different scenarios regarding both the WSS and power network to suggest the best cases for operational cost reduction and energy policies, respectively. Finally, we conclude with the key remarks and future work in Section 7.

2 Proposed framework

As illustrated in Figure 1, the proposed model follows a two-step structure. First, the operational model for the water pump scheduling problem is solved, incorporating robust constraints to account for water uncertainty. Subsequently, the optimal solution of the power and the robust water demand Δd required to operate the WSS are introduced as parameters for the second step.

In the second step, the model addresses the issue of providing demand response to the power system by utilising the pumping stations as flexible sources. This step involves solving a stochastic problem in a deterministic manner by using the expected value of the uncertainty spot prices [49, 50], which represents the price paid to the WSS operator for delivering the service. For the uncertain spot prices, two approaches were taken:

- We analysed the days of the season with the maximum, medium, and minimum average daily costs.

- We used kmeans clustering to identify three clusters representing maximum, medium, and minimum costs and selected the real days closest to the centroid of each cluster.

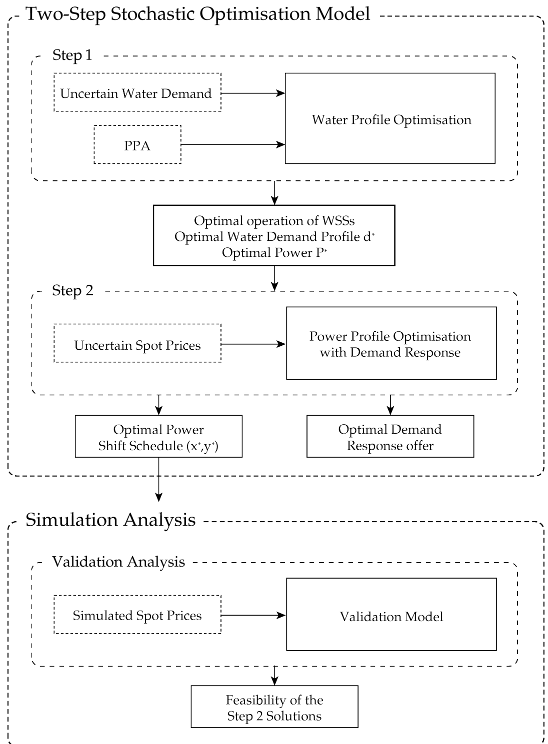

Figure 1: Proposed two-step stochastic optimisation model with an additional feasibility check step.

Finally, the simulation analysis verifies the quality of the solutions from the second step and is verified by repeatedly solving the demand response model with varying simulated spot prices but a single scenario [50–52]. The validation model uses the optimal water pump scheduling and optimal demand response delivery parameters obtained from the second step, and the optimal water profile from the first step.

Subsequently, we analysed different scenarios of this model by varying the season of the year, the delta demand, and the minimum reservoir level tolerated by the WSS operator. Additionally, we examined the impact of three distinct power purchase agreements (PPAs), using the following approaches for PPA prices:

- The average price per hour per season.
- The Chilean National Energy Agency (CNE) curve divides the day into three blocks of minimum, medium, and maximum prices, taking the average price for each block per season.
- The day quarters approach, which takes the average price of the hours per quarter.

3 Operational model for WSSs

This section presents the operational model for the water pump scheduling problem with uncertain water demand in the mine nodes. We introduce the operational constraints for flow, pressure, pipes, pumps, and tanks. Some of the operational equations have a nonlinear and nonconvex nature, so in Section 5, we used different approaches to handle the computational challenge produced by these constraints proposed by [3].

The decisions of this problem are binary variables that determine the water pump status and continuous variables associated with the water demand uncertainty, water flow in the WSS, the water pump power consumption, and the head pressure in each node. The uncertain nature of this problem is related to the stochastic hydro outflows. Therefore, the main goal of this problem is to find the optimal water pump scheduling and the optimal power needed for the operation under a robust scenario for the water demand uncertainty using different electricity tariffs over the year's seasons while minimising the total operational cost of the WSSs [3].

The WSS is formulated as a directed acyclic graph (DAG) $G = (N, A)$ with nodes N and arcs A. Nodes can be categorised as junctions $j \in J$, reservoirs $j \in R$, tanks $j \in S$, mines $j \in M$, or desalination plants $j \in RO$, that is, $N = J \cup R \cup S \cup M \cup RO$. Arcs can be pipes $a \in Pi$ or pumps $a \in Pu$, that is, $A = Pi \cup Pu$.

Following [32] definition for water storage, this article's main distinction between tanks and reservoirs is that tanks allow bidirectional flow whereas reservoirs model the water supply source (i.e., mine water source). Tanks are normally modelled as nodes, as per this paper, but can also be treated as arcs [44].

As in [3], the WSSs in this study work as follows: firstly, the water is desalinated and injected into the network to be stored and pumped into the following pumping stations until they reach the demand nodes. Taking into account the speed, the time blocks when the water is flowing, and the design of these WSSs, the flow reaches a quasi-stationary status, so there is no need to use partial differential equations to the model, and the equations presented in this section represent the physical phenomena of the water pump scheduling problem for WSSs adequately.

The combinatorial nature of this problem can lead to computationally intensive calculations if certain simplifications are not applied. Additionally, the operational nature of the problem introduces time indexes to the variables and parameters.In principle, time is continuous $t \in [0, T] \subset \mathbb{R}$; however, for model tractability, it is discretised into periods $t \in \{1, \dots, T\}$ of length $\tau \in \{\tau_1, \dots, \tau_T\}$. As noted by [32, 53], this time discretisation is practically motivated by the fact that electricity demand and price forecasts are typically provided in discrete, not continuous, time. Consequently, in this paper, the planning horizon is one day, divided into 24 hourly periods.

We made the following assumptions for this model: i) the water pumps start/stop can be performed instantly without any time delay; ii) the fluid in the WSS is considered incompressible, and changes in volume due to flow through pumps and pipelines can be disregarded; iii) the fluid's physical properties remain constant, and variations in pressure are not taken into account. Pressure distribution along the pipeline is calculated assuming a steady-state process, and any effects of fluid transients in the pipeline are neglected.

3.1 Nodes

Water flow conservation equations

We are modelling this problem as a network; thus, the flow conservation constraint applies: for each node $i \in \mathcal{N}$, the difference between the sum of the pipe flows entering and exiting is equal to the water demand $d_{i,t}$ at the node in time t. In general terms, a positive flow $q_{i,j,t}$ on an arc (i, j) means that it goes from i to $j$in time $t \in T$, whilst a negative value of $q_{i,j,t}$ stands for a flow of amount $|q_{i,j,t}|$ from j to i [3]. It is possible to allow only positive flow values and account for the directions with a binary variable; however, since this is a DAG, the water flows only in one direction. Assuming that the demand must be satisfied at every time, the linear conservation constraint for every node i in desalination plants (1), and for junction nodes, i.e., that not a tank S, reservoir R, desalination plant RO, or mine M in (2) are:

$$\sum_{j:(j,i)\in A} q_{i,j,t} - \sum_{j:(i,j)\in A} q_{i,j,t} \geq d_{i,t} \qquad \forall i \in RO,\ \forall t \in T, \tag{1}$$

$$\sum_{j:(j,i)\in A} q_{i,j,t} - \sum_{j:(i,j)\in A} q_{i,j,t} = d_{i,t} \qquad \forall i \in N \setminus (RO \cup S \cup M),\ \forall t \in T. \tag{2}$$

Note that for this problem, the nodes where desalination plants are, the water flow demand is negative since it is a water input to the network. Also, all the junction nodes in between have either a positive or zero demand.

Water demand uncertainty for mining nodes

As we mentioned before, water is a critical resource for many industries, resulting in multi-million dollar losses if there is no availability of it. Also, some industries are not accountable for how much water they use per hour, which results in an uncertain parameter. Therefore, we modelled the water demand robustly using the proposed structure in [54], by creating a new variable $\Delta d_{i,t}$, which represents the variability of the average demand $d_{i,t}$, and it lives in a bounded region (4)

Therefore, the water flow balance in mining nodes (3) is:

$$\sum_{j:(j,i)\in A} q_{i,j,t} - \sum_{j:(i,j)\in A} q_{i,j,t} = d_{i,t} + \Delta d_{i,t} \qquad \forall i \in M,\ \forall t \in T, \tag{3}$$

$$\underline{d_{i,t}} \leq \Delta d_{i,t} \leq \overline{d_{i,t}} \qquad \forall i \in M,\ \forall t \in T, \tag{4}$$

$$\sum_{t\in T}\sum_{i\in M} (\Delta d_{i,t})^2 \leq \gamma_d. \tag{5}$$

where $\underline{d_{i,t}}$ and $\overline{d_{i,t}}$ are the lower and upper bound of the demand variability. Depending on what values the water operator wants to use, one alternative is to utilise a fraction of the average water demand $\underline{d_{i,t}} = -\mu\ d_{i,j}$ and $\overline{d_{i,t}} = \mu\ d_{i,j}$, with $\mu \in [0,1]$, or $\underline{d_{i,t}} = 0$ if it is only interested in the water demand increase scenario. Also, γ_d in (5) represents how much from the mean the variation should live. Also, the way the demand data is used in this case for the mining site nodes, the demand is positive since it corresponds to the water output of the network.

Pressure

The hydraulic head $h_{i,t}$, $i \in N$, is the pressure value expressed as a length in columns of water [m]. In fluid dynamics, the hydraulic head is the total energy per unit weight of fluid and is the sum of the elevation head Z_i, which is the altitude of the node i, $\bar{H}_j$ the pressure in the terminal node j, and the pressure loss $\phi_{i,j,t}$ in the pipeline or pump due to friction [3]. For the WSSs tested in this work, the pressure in the terminal node $\bar{H}_j$ is 0 m under the assumption that every node receiving water has a storage tank exposed to the environment [32, 55].

$$h_{j,t} - h_{i,t} = Z_j - Z_i + \bar{H}_j + \phi_{i,j,t} \qquad \forall (i,j) \in A,\ \forall t \in T. \tag{6}$$

As well as the water flow, the hydraulic head must stay between certain bounds to guarantee the nodes' minimum and maximum pressure levels. Normally, the node potentials are fixed at source nodes, like in the desalination plants in this case, reflecting the fact that at sources, water is not pressurised, but it exploits a fixed geographical height [32]. For all the other nodes, the lower bounds for the hydraulic head are:

$$h_{i,t} = Z_i \qquad \forall i \in RO,\ \forall t \in T, \tag{7a}$$

$$h_{i,t} \geq Z_i \qquad \forall i \in N \setminus RO,\ \forall t \in T. \tag{7b}$$

The bounds of the difference of the hydraulic head for tanks, pipes, and pumps are explained in the next sections.

Tanks

Tanks can make the operation of the network more flexible. In a dynamic setting, where the demand at consumer nodes can vary in time, water can be stored in a tank during a period of low demand and extracted from it to satisfy peak demands.

$$\sum_{j:(j,i)\in A} q_{i,j,t} - \sum_{j:(i,j)\in A} q_{i,j,t} = e_{i,t} \qquad \forall i \in S \cup R,\ \forall t \in T-1, \tag{8}$$

$$e_i^t = \frac{1}{\tau_t}\left(h_{i,t+1} - h_{i,t}\right) A_i \qquad \forall i \in S \cup R,\ \forall t \in T-1, \tag{9}$$

$$h_{i,t} \leq Z_i + \bar{h_i} \qquad \forall i \in S \cup R,\ \forall t \in T, \tag{10}$$

$$h_{i,t} \geq Z_i + \bar{h_i}\gamma_i^{min} \qquad \forall i \in R,\ \forall t \in T, \tag{11}$$

$$h_{i,1} \leq h_{i,T} = Z_i + \bar{h_i}\gamma_i \qquad \forall i \in S \tag{12}$$

with e_i^n denoting the variable volumetric tank inflow, A_i being the cross-sectional area of the tank, τ_t is a time scalar, $\bar{h_i}$ is the tank height, γ_i is the initial and final percentage of the water tank level, and γ_i^{min} is the minimum water tank level percentage during the operation. Equations (8) and (9) represent the water flow balance in tanks, which depends on its volume. To bound the maximum pressure measure in the altitude of the tanks, and since they don't allow water overflow and they are open, we need the Equation (10). Usually, constraint (11) is used to set the minimum water level of a tank or reservoir during the pump scheduling operation, especially if the water operator requires a conservative volume reserved in the tank or reservoir to supply the industry in case of an energy shortage or any event that would stop the water supply for a few hours or days. Industries normally require this constraint because the cost of stopping their operation due to water shortage can cost millions every hour. Finally, Equation (12) is used to set the initial value equal to the previous day's final.

Reservoirs

As previously explained, the main difference between tanks and reservoirs is that tanks allow bidirectional flow, whereas reservoirs represent the water supply source. This is because, normally, reservoirs are fed by natural sources such as rivers or glaciers and thus are assumed to have an infinite supply. Without loss of generality, we assume that reservoirs are infinite sources of water and that the pressure head at each reservoir$r \in R$ is zero; in other words, the total head at reservoir r only represents the elevation head [56]. In this work, the "reservoirs" are, in fact, large tanks located next to the mining site, supplied solely by the desalinated WSS.

3.2 Arcs

Flow bounds

The water pipes are designed to resist a certain flow capacity, which is bounded by its maximum capacity. This bound depends on the pipe's cross-sectional area and the maximum linear velocity $v_{i,j,t}^{\max}$ over time t. [32, 57], and [58] emphasise that this parameter must not exceed a specific value to avoid a number of potential operating problems, for instance, the flow-assisted corrosion problem. Therefore, the maximum flow can be written as

$$\begin{aligned} q_{i,j,t}^{\max} &= Area_{i,j}\ v_{i,j,t,t}^{\max} \\ &= \frac{\pi}{4} D_{i,j}^2 v_{i,j,t,t}^{\max} \qquad \forall (i,j) \in A,\ \forall t \in T. \end{aligned} \tag{13}$$

The flow bounds are for a directed graph, like the WSS we are modelling:

$$0 \leq q_{i,j,t} \leq q_{i,j,t}^{\max} \qquad \forall (i,j) \in A,\ \forall t \in T. \tag{14}$$

where $D_{i,j}$ is the diameter of the pipe (i,j).

Energy loss in pipes

The arcs in a WSS represent pipes in which water is transported from one node to another. In models that don't have stationary status, the flow changes at the beginning and end of a pipe [44]. However, the flow is constant throughout the pipe since we work with a quasi-stationary network. The fundamental equation for a pipe (i,j) is the head-loss equation, also denominated potential-flow coupling constraint in [59], that is regularly of the form

$$h_{j,t} - h_{i,t} = \Delta Z_{i,j} + \Phi_{i,j,t}\left(q_{i,j,t}\right) \qquad \forall (i,j) \in Pi,\ \forall t \in T, \tag{15}$$

where $\Phi_{i,j,t} : \mathbb{R} \to \mathbb{R}$ is a strictly increasing uneven function, concave on the negative half-axis of its domain and convex on the positive half-axis. The flow is not linear in arcs due to the friction modelling in the pipes. A positive flow as a function of the potential difference is strictly increasing but concave: higher flow values mean a higher influence of friction. The other way round, for the same reason, a positive potential loss as a function of the flow is strictly increasing and convex. Equation (15) is also referred to as the potential-loss equation because it describes the pressure loss along a pipe.

Commonly used forms of the head-loss equation are the Darcy-Weisbach equation and the Hazen-Williams equation. Both formulations include constants such as the gravitational acceleration g, the pipe length $L_{i,j}$, and the pipe material roughness coefficient or friction factor [32, 44]. In this case, we used the Darcy-Weisbach equation for its structure, as it is more suitable for the optimisation model.

Since the graph studied in this work is directed, i.e. $q_{i,j,t} \geq 0$, the sign$\left(q_{i,j,t}\right)$ is set to one:

$$h_{j,t} - h_{i,t} = \Delta Z_{i,j} + \frac{8 L_{i,j} f}{\pi^2 g D_{i,j}^5} q_{i,j,t}^2 \qquad \forall (i,j) \in Pi,\ \forall t \in T, \tag{16}$$

where f is the Darcy friction factor.

Note that if the final node j is a tank, then $\Delta Z_{i,j} = \Delta Z_{i,j} + \bar{h_j}$ includes the tank height.

Energy loss in pumps

In pressurised networks, water flows from points of high to low pressure. Hence, increasing the pressure at certain parts of the network is necessary to pump water upstream in a WSS. To represent the status of the pumps, we introduce a binary variable $x_{i,j,t} \in 0, 1$, which indicates if pump $(i,j) \in Pu$ is active or not in time $t \in T$. Active pumps increase the hydraulic head by some controlled non-negative amount represented by the characteristic pump curve:

$$h_{j,t} - h_{i,t} = \alpha_{i,j} - \beta_{i,j} q_{i,j,t}^{\gamma_{i,j}} \qquad \forall (i,j) \in Pu,\ \forall t \in T, \tag{17}$$

where $\alpha_{i,j} > 0$ is the maximum possible pressure increase of the pump $(\Delta Z_{i,j})$, $\beta_{i,j} > 0$ and $\gamma_{i,j} \geq 1$ are pump-specific efficiency parameters [44].

As pumps behave like pipes in the energy loss and since the graph studied in this work is a DAG, i.e. $q_a \geq 0$, and $x_a \in \{0, 1\}$ indicates the state of the water pump, then the Darcy-Weisback equation and the linear equation (17) with $\gamma_{i,j} = 1$ are:

$$\underline{M}(1 - x_{i,j,t}) \leq h_{j,t} - h_{i,t} - (\Delta Z_{i,j} - \beta_{i,j} q_{i,j,t}) \leq \overline{M}(1 - x_{i,j,t}) \qquad \forall (i,j) \in Pu,\ \forall t \in T, \tag{18}$$

$$q_{i,j,t}^{min} x_{i,j,t} \leq q_{i,j,t} \leq q_{i,j,t}^{max} x_{i,j,t} \qquad \forall (i,j) \in Pu,\ \forall t \in T \tag{19}$$

where f is the Darcy friction factor, and $\underline{M} = h_j^{min} - h_i^{max}$ and $\overline{M} = h_j^{max} - h_i^{min}$ [44].

The Equation (18) is one of the most common approaches used for pump head loss. It is derived from (17) with quadratic term $\gamma_{i,j} = 2$. However, the coefficient next to the quadratic term is usually small and negative [60]. Therefore, like in [61] and [46], we neglect the quadratic term since its contribution is small compared to the linear term, and we approximate the pump hydraulic function with energy loss as described in (18).

To link the binary variable $x_{i,j,t}$ and the water flow $q_{i,j,t}$, we use the constraint (19). If the water pump is turned off, i.e. $x_{i,j,t} = 0$ and $q_{i,j,t} = 0$, then the pressure difference $h_j - h_i$ is arbitrary. Here, the value of $q_{i,j,t}^{\min} > 0$ is the minimal relevant non-zero flow; this means that a flow less than $q_{i,j,t}^{\min}$ implies that the pump is inactive ($x_{i,j,t} = 0$), and a positive flow of more than $q_{i,j,t}^{\min}$ makes the pump active ($x_{i,j,t} = 1$).

Finally, for a fixed-speed water pump, the water flow is fixed; therefore,

$$q_{i,j,t} = q_{i,j,t}^{m\bar{a}x} x_{i,j,t} \qquad \forall (i,j) \in Pu_{fixed},\ \forall t \in T, \tag{20}$$

where $q_{i,j,t}^{m\bar{a}x}$ is the maximum water flow in the water pump. In many cases, it represents the water supply provided by a source: for example, in the WSS with desalination plants, the water flow could be the supplied water by the desalination plant since they normally process water in step function curves, given by the number of filters.

Pump power

For a pump with $\eta_{T^\circ\mathrm{C}}$ combined efficiency of the pump and prime mover, and $\rho_{T^\circ\mathrm{C}}$ the water density that depends on the hourly temperature, its power consumption (Mixed Integer Nonlinear Programming - MINLP) is a function of its head gain and water flow rate in MW:

$$P_{i,j,t} = \frac{\rho_{T^\circ\mathrm{C}}\ g}{\eta_{T^\circ\mathrm{C}}} q_{i,j,t}\ (h_{j,t} - h_{i,t})\ 10^{-6} \qquad \forall (i,j) \in Pu,\ \forall t \in T. \tag{21}$$

The water pump efficiency $\eta_{T^\circ\mathrm{C}}$ is determined by its manufacturer. It is a fixed value in the temperature range for which it was built: when the temperature is out of the optimal range, the efficiency decreases. Furthermore, the pump efficiency is affected by the water flow [62, 63]; nevertheless, for the purpose of this work, we assume that the water flow does change its efficiency. Also, the water density varies according to the temperature regardless of the other factors. Generally, it is assumed that the temperature is such that the water density $\rho = 1000\ Kg/m^3$, which is 4°C [64, 65]. However, we assume that since the temperature doesn't normally go below zero or above 40°C, then the pressure of the water doesn't change significantly to include that in the model.

3.3 Objective function

The objective function seeks to minimise the cost of operation and the on/off penalty of the water pumps. Let X be the space of all the optimisation variables of the problem, and $T = 25$ hours to adjust the 24-hour cycle; therefore, the objective function is:

$$f(X) = \sum_{(i,j)\in Pu} \sum_{t=1}^{T-1} \left(P_{i,j,t} C_t + |x_{i,j,t+1} - x_{i,j,t}| C_m\right), \tag{22}$$

where C_t is the cost of electricity in having a pump on during time t, normally determined by a PPA with a power generator, and C_m is the penalty for a single pump switch. The value of C_m is based on recommendations by [66], which consists of iterating over different values of C_m and picking one that is reasonable for the electricity prices that allows the switching of the pumps. This is in case there is no data for the future pumping station maintenance costs.

The pump switching can negatively affect a system's maintenance cost due to the changing loads contributing to fatigue-related failures [18]; thus, penalising the pump switching often reduces this negative impact and accounts for maintenance costs [67, 68].

Another way to represent the pump maintenance penalty is using a quadratic term instead of the absolute value: $\sum_{(i,j)\in Pu}\sum_{t=1}^{T-1}(x_{i,j,t+1} - x_{i,j,t})^2$ [69]. Both approaches are equivalent and nonlinear; however, the absolute value has fewer added constraints in the exact reformulation, which we explain in the next section.

3.4 Water profile optimisation

Therefore, the optimisation model for the water profile and optimal power, known in the literature as the water pump scheduling problem, is the following:

$$\begin{aligned} &\min\,(22) \qquad (23)\\ \text{s.t.}&\\ &(1) - (5)\\ &(7) - (14)\\ &(16), (18), (19), (21) \end{aligned}$$

4 Demand response

As we explained before, once we solved the operational model for the WSS, we used the optimal power per hour as input for the demand response model. This provides a baseline to determine when the WSS could bid and provide flexibility to the power system.

For the Chilean regulation [70, 71], there are five different ancillary services that electricity clients can provide to the power network: fast (CRF), primary (CPF), secondary (CSF), tertiary (CTF) control of frequency, and interruptible charges (CI). The fast, first and second control of frequency requires an activation time between 1 second and 5 minutes, making it almost impossible for the pumping system to react and to function in a steady state condition. Also, the interruptible charges, which almost never happen because the reward is too low, require an activation time of 30 minutes and a minimum delivery time of 2 hours, as we can see in Table 1.

Table 1: Characteristics of the frequency control time dispatch of the different ancillary services regulated in Chile. Fast control of frequency (CRF), Primary control of frequency (CPF), Secondary control of frequency (CSF), Tertiary control of frequency (CTF), and Interruptible charges (CI) [70, 71].

Ancillary Service	Start Activation	Total Activation	Min Delivery	Max Delivery
CRF	-	1 s	5 min	-
CPF	-	10 s	5 min	-
CSF	-	5 min	15 min	-
CTF	**5 min**	**15 min**	**-**	**1 hr**
CI	-	30 min	2 hr	-

On the other hand, the tertiary control of frequency instruction is given in real-time and requires an activation time of 15 minutes and a maximum delivery time of 1 hour, which makes it an ideal candidate for the WSSs. However, for this study, we assume that the start time for the CTF occurs at the beginning of a certain hour and that there is no maximum delivery time. As energy-intensive infrastructures, WSSs could potentially provide significant amounts of demand response, as discussed in the results section. Therefore, new energy policies could be developed to address their characteristics and incentivise their participation in the capacity market. We also assume that no payment is made for being available on the capacity market; the financial reward is based solely on the difference between the spot and PPA prices. The maximum delivery time can be constrained using a modified version of Equation (31), as we explain later in this work.

It is sensible to incorporate into the model the uncertainty of the spot prices for which the DR service is being paid to the WSS operator. We based our model on the two-step framework proposed by [19], which incorporates a water demand forecast in the first step and an electricity price forecast in the second step. However, in our case, we included the binary variable that returns the water pump scheduling $x_{i,j,t}$, and incorporated an additional step to validate the solutions given by the second step.

For this purpose, we introduce the set of scenarios $s \in S$, which depends on the spot prices $r_{t,s}$ in \$/MWh [50, 52], and calculate the new objective function using the expected value and the price structure proposed by [2, 19]:

$$\begin{aligned} f^{DR}(X) =& \mathbb{E}(\text{Operational Cost} - \text{DR Benefit}) \\ =& \sum_{s\in\mathcal{S}} \sum_{t=1}^{T-1} \Bigg(\sum_{(i,j)\in Pu} (P_{i,j,t,s} C_t + |x_{i,j,t+1} - x_{i,j,t}| C_m) \\ & - \left(P^{SH}_{t,s} C_t - P^{DR}_{t,s} r_{t,s}\right) \Bigg) p_s, \end{aligned} \tag{24}$$

where p_s is the occurrence probability of the scenario s, $P^{SH}_{t,s}$ corresponds to the shifted load or recovery of the electric power of the DR block provided in another period t in MW, and $P^{DR}_{t,s}$ corresponds to the electric power of the DR block put on sale through a bid on the spot market at period t in MW. Mkireb et al. [2] explains that using the spot price $r_{t,s}$ for the DR provision is reasonable for the French system because it allows the arbitrage of prices and to offer the service at the most convenient time for the WSS. Also, they assumed that the power recovery pays the agreed PPA price.

Also, the following constraints are needed to provide DR to the grid:

$$\sum_{(i,j)\in Pu} P_{i,j,t,s} \geq \sum_{(i,j)\in Pu} P^{*}_{i,j,t} + P^{SH}_{t,s} - P^{DR}_{t,s} \qquad \forall s \in S,\ \forall t \in T, \tag{25}$$

$$P^{DR}_{min}\ y_t \leq P^{DR}_{t,s} \leq P^{DR}_{max}\ y_t \qquad \forall s \in S,\ \forall t \in T, \tag{26}$$

$$P^{SH}_{min}\ (1-y_t) \leq P^{SH}_{t,s} \leq P^{SH}_{max}\ (1-y_t) \qquad \forall s \in S,\ \forall t \in T, \tag{27}$$

$$\sum_{t\in T-1} P^{SH}_{t,s} = \sum_{t\in T-1} P^{DR}_{t,s} \qquad \forall s \in S, \tag{28}$$

$$\sum_{t\in T-1} \sum_{(i,j)\in Pu} P_{i,j,t,s} = \sum_{t\in T-1} \sum_{(i,j)\in Pu} P^{*}_{i,j,t} \qquad \forall s \in S. \tag{29}$$

where y_t is a binary variable indicating the position taken on the spot market at period t whether to provide DR or not, $P^{max}_{i,j,t}$ is the maximum power of the water pump (i,j) in time t, and for both, the maximum power for DR and the recovery SH, is $P^{DR}_{max} = P^{SH}_{max} = \sum_{(i,j)\in Pu} P^{max}_{i,j,t}$ and $P^{*}_{i,j,t}$ is the optimal power of the operational model (23). Unlike the optimisation framework proposed by [47], we let the model decide when to provide DR, and we do not restrict it to certain hours and duration of the DR event. In this case, we are assuming that all the WSS nodes are connected only to one bus of the electrical grid; however, this is not always true. Therefore, it is left as proposed future work.

In addition to these constraints, the water flow $q_{i,j,t,s}$ and the pressure $h_{i,t,s}$ now have the scenario index. Furthermore, the pump power (21) needs to be relaxed for the DR model, but it is worth mentioning that the bounds are kept tight:

$$P_{i,j,t,s} \leq \frac{\rho_{T^\circ\mathrm{C}}\ g}{\eta_{T^\circ\mathrm{C}}} q_{i,j,t,s}\ (h_{j,t,s} - h_{i,t,s})\ 10^{-6} \qquad \forall (i,j) \in Pu,\ \forall t \in T,\ \forall s \in S. \tag{30}$$

Other electrical operational constraints have been proposed for DR models. In [2] presented a DR model for the French ancillary services mechanism, which has a maximum of two blocks where they can bid to provide DR, and the duration between two DR bids must not be less than the maximum duration of the two bids. For example, to represent that in 3 periods, a maximum of two blocks can be used, the constraint is:

$$y_t + y_{t+1} + y_{t+2} \leq 2 \qquad \forall t \in T-2 \tag{31}$$

4.1 Power profile optimisation with demand response

Therefore, we formulate a two-step model optimisation problem that is solved in one instance, where the first stage corresponds to the decision variables of water pump scheduling $x_{(i,j),t}$, and the demand response scheduling y_t; and second stage, the water flow q, head pressure h, power used P, demand response power provided P^{DR}, and the recovered power P^{SH} which depends on the spot price scenarios. The model for Power Profile Optimisation with the Demand Response for the water pump scheduling problem is the following:

$$\begin{aligned} &\min\,(24) \\ \text{s.t.}& \\ &(1) - (5) \\ &(7) - (14) \\ &(16),\,(18),\,(19),\,(30) \\ &(25) - (29) \end{aligned} \tag{32}$$

5 Alternative models for the WSS operation

This section presents three methodologies to handle the nonlinearities present in the original problem, as we explained in Section 3, whose main differences lie in the final nature of the model, linear or nonlinear. We describe the three proposed models: the fixed flow model, the semi-linear model and the binary expansion approach model. Additionally, we discuss the theoretical and practical advantages and disadvantages of each model, and we compare them using computational experiments in Section 6.

5.1 Reformulation techniques to solve the complicating constraints

To handle the complicating nonlinear and nonconvex constraints, we consider the following reformulation techniques:

1. **Reformulating the binary and continuous products:** We use an auxiliary variable z to linearise $z = x \cdot y$ where x is binary and y is a continuous variable such that $y \in [0, b]$. The following formulation is applied:

$$z \leq y, \quad z \leq x \cdot b, \quad z \geq y + b \cdot (x-1). \tag{33}$$

2. **Reformulating the absolute value of binary variables:** We use an auxiliary variable w to linearise $w = |x - y|$ where x and y are binary variables. An analogous expression for w is $w = |x-y| = \max\{x-y, y-x\}$, therefore, the following formulation is applied:

$$w \geq x - y, \quad w \geq y - x. \tag{34}$$

Using the expression (34) for the pump maintenance penalty in the objective function of the step 1 model $f(X)$ with $B_{i,j,t} = |x_{i,j,t+1} - x_{i,j,t}|$:

$$f'(X) = \sum_{(i,j)\in Pu} \sum_{t=1}^{T-1} \left(P_{i,j,t}C_t + B_{i,j,t}C_m\right), \tag{35}$$

and for the step 2 model is:

$$f'^{DR}(X) = \sum_{s\in\mathcal{S}} \sum_{t=1}^{T-1} \Bigg(\sum_{(i,j)\in Pu} (P_{i,j,t,s}C_t + B_{i,j,t}C_m) - \big(P^{SH}_{t,s}C_t - P^{DR}_{t,s} r_{t,s}\big) \Bigg) p_s, \tag{36}$$

and adding the constraints:

$$B_{i,j,t} \geq x_{i,j,t+1} - x_{i,j,t} \qquad \forall (i,j) \in Pu,\ \forall t \in t \in T-1, \tag{37a}$$

$$B_{i,j,t} \geq -(x_{i,j,t+1} - x_{i,j,t}) \qquad \forall (i,j) \in Pu,\ \forall t \in T-1, \tag{37b}$$

3. **Binary expansion approach:** We discretise a continuous variable $x \in [x_{LB}, x_{UB}]$ [3, 72, 73]:

$$x = x_{LB} + \frac{x_{UB} - x_{LB}}{2^N - 1} \cdot \sum_{i=1}^{N} 2^{i-1} \cdot x_i, \tag{38}$$

where x_i is the binary variable that determines the values of the binary division of x.
The binary expansion approach for the water flow variable $q_{i,j,t}$ is:

$$q_{i,j,t} = \frac{q^{max}_{i,j,t}}{2^K - 1} \sum_{l=1}^{K} 2^{l-1}\ q_{l,i,j,t} \qquad \forall (i,j) \in A,\ \forall t \in T. \tag{39}$$

The same approach can be applied to the product of continuous variables using the binary expansion approach in one of the variables, and the other variable is left as it is. Then, we have the product of a binary and continuous variable; therefore, we can apply Equation (33). So, to linearise the bilinear product $x \cdot y$, we define the variable $z_i = x_i \cdot y$, and use Equation (33) with a Big M:

$$x \cdot y = x_{LB} \cdot y + \frac{x_{UB} - x_{LB}}{2^N - 1} \sum_{i=1}^{N} 2^{i-1}\ z_i, \tag{40a}$$

$$0 \leq y - z_i \leq M\ \ (1 - x_i) \qquad \forall i \in N, \tag{40b}$$

$$0 \leq z_i \leq M\ x_i \quad \forall i \in N. \tag{40c}$$

Applying the reformulation to the energy loss constraint in pipes (16) using $z_{k,i,j,t} = q_{k,i,j,t} \cdot q_{i,j,t}$, with $q_{k,i,j,t}$ the binary variable for the partition of $q_{i,j,t}$, and $q_{LB} = 0$, $M = q_{UB} = q^{max}_{i,j,t}$, and (39), then the energy loss in pipes is:

$$h_{j,t} - h_{i,t} = \Delta Z_{i,j} + \frac{8 L_{i,j} f}{\pi^2 g} \frac{q^{max}_{i,j,t}}{2^K - 1} \sum_{k=1}^{K} 2^{k-1}\ z_{k,i,j,t} \qquad \forall (i,j) \in Pi,\ \forall t \in T, \tag{41a}$$

$$0 \leq \frac{q^{max}_{i,j,t}}{2^K - 1} \sum_{l=1}^{K} 2^{l-1}\ q_{l,i,j,t} - z_{k,i,j,t} \leq q^{max}_{i,j,t}\ (1 - q_{k,i,j,t}) \qquad \forall (i,j) \in Pi,\ \forall t \in T,\ \forall k \in N, \tag{41b}$$

$$0 \leq z_{k,i,j,t} \leq q^{max}_{i,j,t}\ q_{k,i,j,t} \qquad \forall (i,j) \in Pi,\ \forall t \in T,\ \forall k \in N, \tag{41c}$$

Similarly, as in equation (38), we apply the binary expansion approach to the linear energy loss constraint in pumps (18), and in all the other constraints that have $q_{i,j,t}$, using Equation (39):

$$\underline{M}(1 - x_{i,j,t}) \leq h_{j,t} - h_{i,t} - \Bigg(\Delta Z_{i,j} - \beta_{i,j} \frac{q^{max}_{i,j,t}}{2^K - 1} \sum_{l=1}^{K} 2^{l-1}\ q_{l,i,j,t} \Bigg) \leq \overline{M}(1 - x_{i,j,t}) \qquad \forall (i,j) \in Pu,\ \forall t \in T. \tag{42}$$

We also apply the binary expansion approach (40) to the pump power constraint (21) using $p_{k,i,j,t} = q_{k,i,j,t}\ (h_{j,t} - h_{i,t})$, and $q_{LB} = 0$, $q_{UB} = q^{max}_{i,j,t}$, and $M = \max\{Z_i, Z_j\}$:

$$P_{i,j,t} = \frac{\rho\ g}{\eta}\ \frac{q^{max}_{i,j,t}}{2^N - 1}\ \sum_{k=1}^{N} 2^{k-1}\ p_{k,i,j,t}\ 10^{-6} \quad \forall (i,j) \in Pi,\ \forall t \in T, \tag{43a}$$

$$0 \le h_{j,t} - h_{i,t} - p_{k,i,j,t} \le \max\{Z_i, Z_j\}\ (1 - q_{k,i,j,t}) \quad \forall k \in N,\ \forall (i,j) \in Pi,\ \forall t \in T, \tag{43b}$$

$$0 \le p_{k,i,j,t} \le \max\{Z_i, Z_j\}\ q_{k,i,j,t} \quad \forall k \in N,\ \forall (i,j) \in Pi,\ \forall t \in T. \tag{43c}$$

Similarly, for the relaxed power constraint of the DR model (30), using the same structure as in (43), we have:

$$P_{i,j,t} \le \frac{\rho\ g}{\eta}\ \frac{q^{max}_{i,j,t}}{2^N - 1}\ \sum_{k=1}^{N} 2^{k-1}\ p_{k,i,j,t}\ 10^{-6} \quad \forall (i,j) \in Pi,\ \forall t \in T, \tag{44a}$$

$$0 \le h_{j,t} - h_{i,t} - p_{k,i,j,t} \le \max\{Z_i, Z_j\}\ (1 - q_{k,i,j,t}) \quad \forall k \in N,\ \forall (i,j) \in Pi,\ \forall t \in T, \tag{44b}$$

$$0 \le p_{k,i,j,t} \le \max\{Z_i, Z_j\}\ q_{k,i,j,t} \quad \forall k \in N,\ \forall (i,j) \in Pi,\ \forall t \in T. \tag{44c}$$

5.2 Alternative models

Like in [3], we proposed two alternatives for the original water profile optimisation (23) and the power profile optimisation with demand response (32) to analyse the computational effectiveness of the binary expansion approach method compared to other classic approaches. The first approach is the semi-linear "SL", which linearises the binary and continuous products in the problem's constraints. The second alternative is the binary expansion approach "BEA"; it linearises the binary and continuous products and the complicating variables of water flow and pump power.

Model 1: SL (MINLP)

The semi-linear model (SL) only linearises the binary and continuous products using the (34) technique in equation (22) but leaves the pump power constraint bilinear and the energy loss equation in pipes quadratic. This method removes the complexity derived from the binary product in the problem's constraints. This model is still MINLP because of the bilinear term in the pump power constraint and the quadratic water flow in the energy loss equation.

The SL optimisation model for the Water Profile Optimisation of step 1 is:

$$\min\ (35) \tag{45}$$

s.t.

(1) – (5)

(7) – (14)

(16), (18), (19), (21)

(37)

The SL optimisation model for the Power Profile Optimisation with Demand Response of step 2 is:

$$\begin{aligned}
&\min\,(36) \\
\text{s.t.}& \\
&(1) - (5) \\
&(7) - (14) \\
&(16),\ (18),\ (19),\ (30) \\
&(25) - (29) \\
&(37)
\end{aligned} \tag{46}$$

Model 2: BEA (MILP)

The binary expansion approach model BEA considers the linearisation of the binary and continuous products using the (34) technique, and the bilinear products and quadratic elements using the binary expansion approach (38) and (40) in all the constraints where $q_{i,j,t}$ and $P_{i,j,t}$ are present. It is worth mentioning that the computational efficiency of the binary expansion approach is highly dependent on the number of partitions N taken. The higher this number is, the more accurate it should be; however, the longer it takes to solve. This is because 2N equations are added to the optimisation model for every constraint where this technique is used. The optimisation model is:

The BEA optimisation model for the Water Profile Optimisation of step 1 is:

$$\begin{aligned}
&\min\,(35) \\
\text{s.t.}& \\
&(1) - (5) \\
&(7) - (14) \\
&(41),\ (42),\ (19),\ (43) \\
&(37),\ (39)
\end{aligned} \tag{47}$$

The BEA optimisation model for the Power Profile Optimisation with Demand Response of step 2 is:

$$\begin{aligned}
&\min\,(36) \\
\text{s.t.}& \\
&(1) - (5) \\
&(7) - (14) \\
&(41),\ (42),\ (19),\ (44) \\
&(25) - (29) \\
&(37),\ (39)
\end{aligned} \tag{48}$$

6 Computational experiments

The proposed framework and models defined in Sections 2 and 5 were tested on realistic high altitude WSS using the Gurobi 10 solver [74] via Julia [75]: the experiments were done using a long and steep network that send desalinated water from the sea level up to the mountains (more than 3000 meters above sea level).

In Figure 2, there is an example of a real WSS that pumps up desalinated water to a mine located at 3100 m.a.s.l. in the Chilean Atacama desert [76]. This water network corresponds to the CODELCO Radomiro Tomic RT WSS tested, and it has one reverse osmosis desalination plant and five interconnected pumping stations, compounded by a water pump and tank, one reservoir and one mine, which has a water demand of 1.5 m^3/s, and a pipe length of 153 km. The data for the nodes and arcs can be seen in Tables A1 and A2.

For the water demand profile, we created a constant one, that changes slightly in the warmer hours of the day, assuming that some evaporation occurs during that time. Therefore, the profile $d_{i,t}$ used in the constraint 3 is the following: q_M m^3/s between 21:00 and 9:00, which is 1.5 for the RT WSS, and a 10% more between 9:00 and 21:00, i.e., 1.65 m^3/s for the RT WSS. Also, for Equation 4, the bounds used were $\underline{d_{i,t}} = -\mu\ d_{i,j}$ and $\overline{d_{i,t}} = \mu\ d_{i,j}$, with $\mu = 10\%$. Finally, the γ_d which determines how much the Δd can deviate in constraint 5. For this purpose, we selected a $\gamma_d = (\gamma \sum_{t \in T} q_M)^2$, with $\gamma = 1\%$ for most of the analysis, with the exception of one of the following sections, where we study the impact of this parameter.

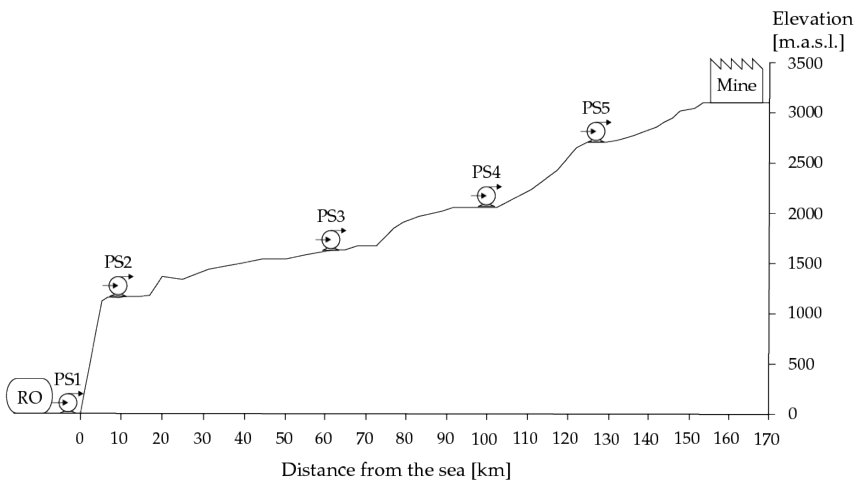

Figure 2: Cross-section of the WSS of Radomiro Tomic (RT) Copper Chilean mine [3].

The values of other parameters for the model were obtained from [76]: pipe maximum speed $v_{max} = 2.5\ m/s$, pipe diameter $D = 1\ m$, Darcy friction factor $f = 0.01$, pump linear parameter $\beta_{i,j,t} = 1/q^{max}_{i,j,t}$ using [46] technique, and the minimum water tank level percentage $\gamma_i^{min} = 80\%$ that depends on the industry, however, we also tested with a 50% to see how the DR model can reduce even more the operational costs. The minimum power to provide DR is $P^{DR}_{min} = 5$ MW and, the minimum power to recover is $P^{SH}_{min} = 0$ MW, and the $P^{max}_{i,j,t}$ was calculated using $q^{max}_{i,j,t}$ and the according Z_i and Z_j.

For the water density ρ(T°C) that depends on the water temperature, we used the data shown in Table A4, according to the season's temperature. Likewise, the pump efficiency varies according to the temperature. In Section 6.4, we explain in detail the assumptions made regarding the temperature. Finally, the electricity prices for the PPA and spot price scenarios were obtained from the Chilean national electrical operator and estimated accordingly, as we explain in Sections 6.1 and 6.3.

The following subsection presents the different computational experiments analysed to understand the efficiency of the proposed method and the key parameters and variables of the water pump scheduling problem with demand response.

6.1 Proposed the PPA tariff C_t

The power purchase agreement (PPA) is a long-term bilateral agreement to purchase clean energy from a specific asset at a predetermined price between a renewable developer and a consumer, which is generally a company requiring large amounts of electricity, or between a developer and a supplier who then resells the energy [77]. PPAs are usually signed for a long-term period between 10-20 years.

Normally, PPA prices vary depending on the season of the year and the renewable energy availability: during winter, the costs rise due to higher demand in the network, and solar power tends to decrease the prices during the day; and during summer, the costs tend to plummet to zero during the day due to the solar power.

The way some PPA work is by fixing an electricity price for some hours in the day or according to the client's needs. It can also be flexibly structured, but the core principle is that a buyer agrees to buy the future energy production of a seller, which, most of the time, offers a renewable source of power generation at an agreed-upon fixed price. PPAs are financially attractive for sellers, providing price certainty, unlike trading in electricity markets. However, PPAs can bring quantity uncertainty for buyers due to the uncertainty of future green energy delivery [78].

Another type of PPA is the Corporate Power Purchase Agreement (CPPA), which is a long-term contract under which a business agrees to purchase electricity directly from an energy generator. This differs from the traditional PPA of buying electricity from licensed electricity suppliers and has more requirements like minimum duration that covers at least the debt term of the project finance. Both methods calculate the price using the levelised cost of electricity (LCOE), which determines the choice of the contract price that affects the payback time and the project profitability. An accurate LCOE evaluation is necessary to support investments in new power plants based on renewable energy sources [79].

In the case of Chile, the National Energy Commission (CNE) is the regulator organisation of the energy sector, and it publishes detailed information about high and low time blocks in the day, energy regulations and electrical tariffs. The CNE has a time block structure with differentiated electricity prices: peak hours (18:00 to 23:00), average hours (7:00 to 18:00) and off-peak hours (23:00 to 7:00), and their prices decrease accordingly [80].

Big companies, like the CODELCO mine, publicly publish their PPAs contract capacity and energy origin, renewable or non-renewable sources; however, the prices are not shown. Therefore, since we don't know the specific values of the PPA signed by CODELCO, we estimated it for each season, taking the average marginal cost per hour as a base point and comparing it using the CNE block time structure and proposed day-quarter time blocks.

Average PPA

First, we created the Average PPA, which corresponds to the hourly average price of all the days of one season. This price will act as a baseline for the other PPAs proposed: CNE blocks and the Quarter blocks. For this purpose, we used the data from one year of the Radomiro Tomic electric bar in the northern region of Chile (Atacama Desert) taken from the marginal costs of the National Electrical Coordinator [81]. We divided the year into four seasons: Winter 2023 (June to August), Spring 2023 (September to November), Summer 2024 (December to February) and Autumn (March to May).

CNE PPA

For the CNE PPA, we utilised the same seasonal data as in the Average PPA, but in this case, we divided each day into three-time blocks, following the CNE recommended price structure. Finally, for each time block, we performed the average, resulting in the fixed price for the block.

Quarter PPA

Lastly, for the proposed Quarter PPA, we divided the day into four-time blocks: (1:00 to 6:00), (7:00 to 12:00), (13:00 to 18:00) and (19:00 to 24:00). Similarly, as in the CNE PPA, for each time block, we calculated the average price per block using the seasonal data.

In Figure 3, we can see in black all the daily marginal cost curves per season, in red the Average PPA, in green the CNE PPA, and in blue the Quarter PPA. One of the most outstanding characteristics shown here is the variable behaviour of the costs in winter, compared to the warmer seasons. Another interesting fact is the lower prices during the day for the warmer seasons, particularly during summer: this is not a surprise because there has been a lot of investment in renewable energies in the north of Chile, especially in solar power, which most of the time plummets the cost to zero for around eight hours per day.

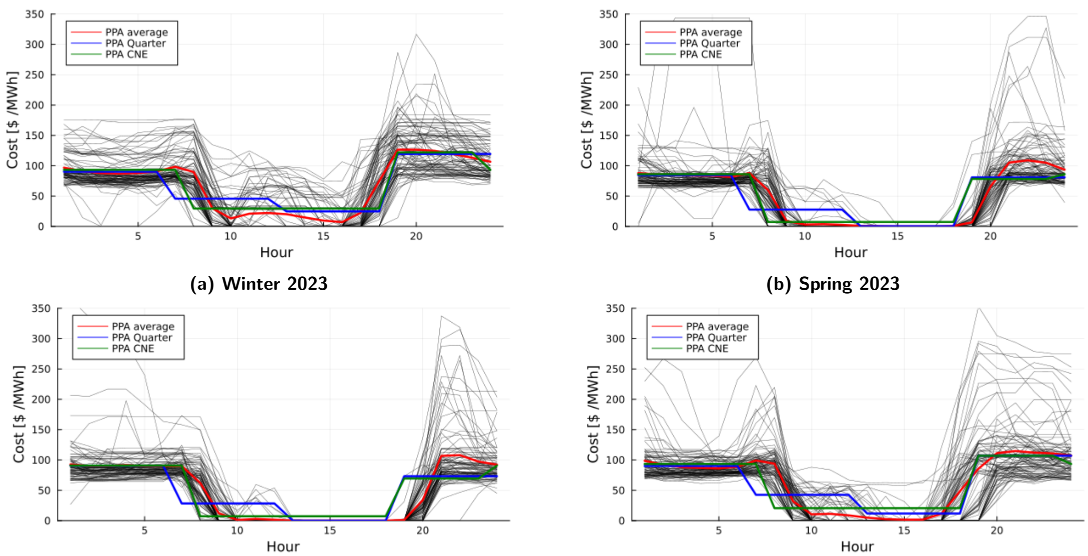

(a) Winter 2023

(b) Spring 2023

(c) Summer 2024

(d) Autumn 2024

Figure 3: Hourly electricity prices of each season in the Radomiro Tomic electric bar in the northern region of Chile (2024). The CNE price, Quarter, and hourly Average are displayed.

6.2 Choosing the appropriate cost of maintenance C_m

As we explained before, the pump switching can negatively affect the water system's maintenance cost C_m due to the changing load contributing to fatigue-related failures [3, 18]. We can calculate C_m by following the recommendations of [66], which consists of trying different values of C_m for a given vector of electricity prices C_t, when the WSS maintenance cost is unknown. In particular, [3] analysed the C_m cost for this work WSSs, finding a balance between the number of times the water pumps could be switched on or off, and the total operational cost: for a 15% of flexibility in the number of active pumps, i.e., for the RT WSS, around 15-18 slots of inactive pumps in total in a 24-hour horizon, the chosen value is $C_m = \$3$. This cost can be updated by creating a correct maintenance optimisation problem and tuning after some maintenance experience.

6.3 Creating the spot prices scenarios

For the spot prices, we tested two types of prices, namely, the extreme cases and the kmeans cases. In both types, we selected three prices: minimum, medium and maximum. Below we explain how we selected the prices.

Extreme cases

As in Section 6.1, we took the marginal cost data from the past year and divided it into seasons. Then, for each season, we calculated the average cost per day, and selected the day with the lowest, medium and highest average. We called these prices "extreme" because they represent the outer bounds of the season.

In Figure 4, the selected minimum, medium and maximum spot prices are shown. Note that winter provides the biggest gap between the minimum and maximum spot prices, and during the warmer seasons, this gap becomes smaller. Also, the PPA Average, almost in all the seasons is between the minimum and maximum extreme spot prices. In summary, this approach gives us a general idea of when could be the best time to provide demand response by looking at the gap between the PPA and the spot price; however, since the weight of each spot price scenario is equal, this could end in optimistic results.

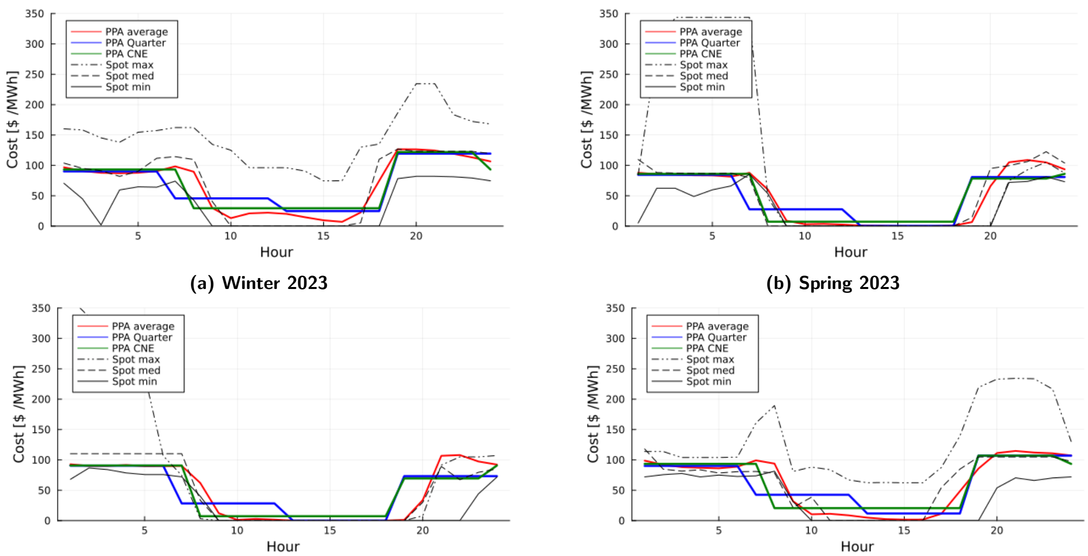

(a) Winter 2023 (b) Spring 2023

(c) Summer 2024 (d) Autumn 2024

Figure 4: Hourly electricity prices of each season in the Radomiro Tomic electric bar in the northern region of Chile (2024). The Extreme Spot prices maximum, medium and minimum are displayed alongside the PPA CNE, PPA Quarter, and PPA Average.

Clustering according to the average daily price

The other way of creating the spot prices is through the kmeans clustering algorithm. For this purpose, we used the kmeans package in Julia, which receives as input the set and the number of clusters and automatically selects with a random function the starting points for each cluster. Like with the extreme cases, we clustered the daily average prices per season in three groups: minimum, medium, and maximum. We also got the size of each cluster, and therefore, we calculated the weight of each group by dividing the cluster size over the total number of days. Since the centroids are non-real data, we selected the day that was closer to the centroid.

In Figure 5, we can see the weights of each cluster per season. In all the seasons, the biggest group is the minimum, with a peak in winter. Also, the medium group increases its size in the warmer seasons, with a peak in summer. Finally, the maximum group remains almost constant during the year, except in spring. This is an important insight since the maximum spot price is the one the WSS operators are looking for due to the gap difference with the PPA prices, and when they can leverage the DR provided to the power system, and therefore reduce their operational costs.

In Figure 6, the selected minimum, medium and maximum spot prices created using the kmeans algorithm are displayed. Like in the extreme spot prices, winter provides the biggest gap between the minimum and maximum spot prices, although smaller in this case, and during the warmer seasons, this gap becomes smaller. Also, the gap between the minimum and maximum prices is smaller compared to the extreme prices. This is because we are taking the centroid of the clusters and not the extreme values. Furthermore, the medium curve is slightly higher with the kmeans algorithm, and for spring and autumn, this approach chooses a spot price with higher values in the evening compared to the extreme values. In summary, this approach gives us a more realistic idea of how the spot prices behave and, thus, end in better results for the DR provision.

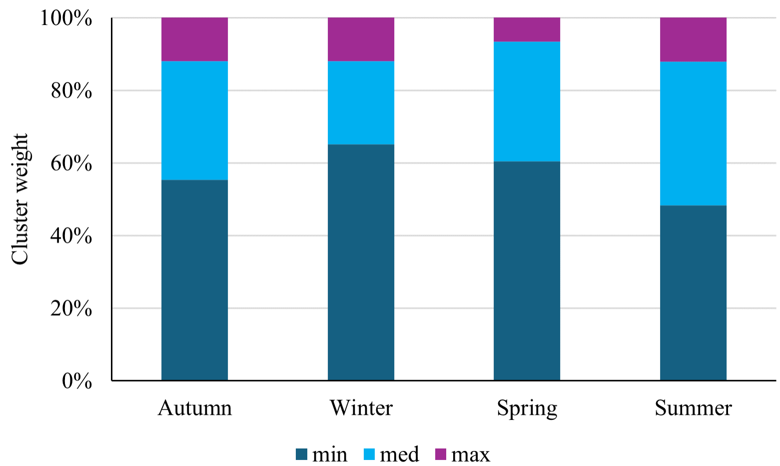

Figure 5: Weights of the spot prices created by the kmeans algorithm per season.

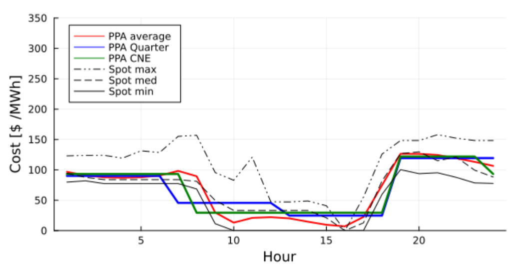

(a) Winter 2023

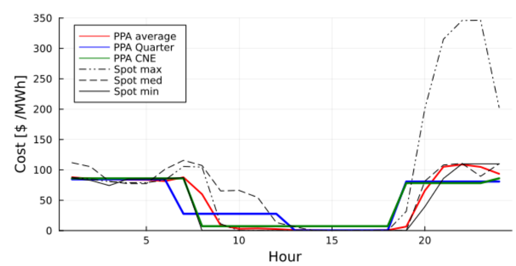

(b) Spring 2023

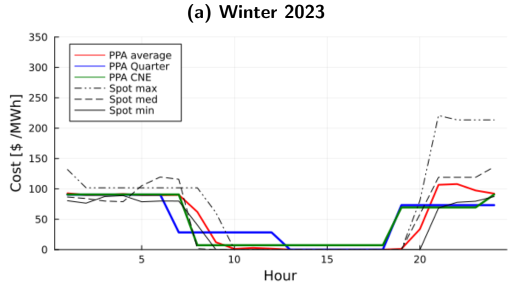

(c) Summer 2024

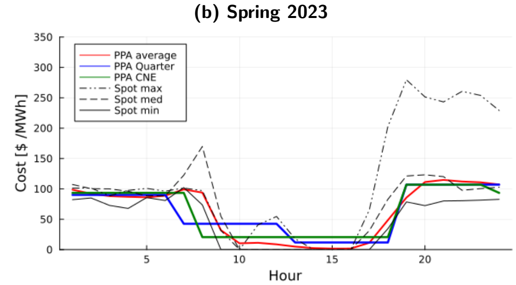

(d) Autumn 2024

Figure 6: Hourly electricity prices of each season in the Radomiro Tomic electric bar in the northern region of Chile (2024). The kmeans Spot prices maximum, medium and minimum are displayed alongside the PPA CNE, PPA Quarter, and PPA Average.

6.4 Temperature per season

As we mentioned in chapter 3.2, the water pump efficiency varies when the temperature is out of the bounds for which it was built. Table 2 shows the 2023 average monthly temperature of Calama, the city where some of the water pumps of the CODELCO WSS are located. For this analysis, we assumed that all the water pumps are subject to the same temperature and that are connected to the same electrical bus. Also, by looking at the average temperature in Table 2, we assumed that the optimal efficiency $\nu = 80\%$ for the range [6°C, 23°C], and that outside that range, the efficiency decreases to $\nu = 70\%$.

Table 2: Average monthly temperature in Calama in 2023 [82].

	Jan	Feb	Mar	Apr	May	Jun	Jul	Aug	Sep	Oct	Nov	Dec
Max	24 °C	24 °C	24 °C	23 °C	22 °C	20 °C	20 °C	21 °C	22 °C	23 °C	24 °C	24 °C
Mean	17 °C	17 °C	16 °C	14 °C	12 °C	11 °C	10 °C	12 °C	13 °C	15 °C	16 °C	17 °C
Min	8 °C	8 °C	7 °C	6 °C	4 °C	3 °C	2 °C	3 °C	4 °C	5 °C	6 °C	7 °C

To simplify the temperature calculations, we used the hourly daily average of March for Autumn, July for winter, October for Spring, and December for summer, as shown in Table A3. Note that the numbers in bold represent the hours when the temperature is out of bounds of the water pump efficiency range previously defined. Finally, with the hourly temperature per season, we can get the water density ρ according to the temperature. In Table A4, we can see the values between 0°C and 100°C [64, 65].

6.5 Comparison of running times

In Table 3, some results for the RT WSS are displayed using the parameters described before, for the MINLP model Semi Linear (SL) and the MILP Binary Expansion Approach (BEA) for the step 2 model. The optimality gap of the MINLP methods is 0.01% in all of the cases. It is worth mentioning that solving the original model (23) and the DR model (32) with the (SL) instance takes too long, in particular for the scenarios in the DR model, so we had to set a 15 minutes time stop to the Gurobi solver in order to add those results to the table. Also, for some cases with the (SL) approach, the 15 minutes wasn't enough to find an optimal solution, thus we stopped trying with this approach. Otherwise, it could have taken more than 7 hours to complete. Also, for this work, we consider that the SL model reaches the optimal value in the water profile optimisation to have a baseline to compare it with the binary approximation (BEA) of the original problem. For the step 2 model, the power profile optimisation with the demand response model is considered to reach optimality.

Table 3: Comparison of the two models using the RT WSS for different cases with their respective PPA price. The Gurobi gap in all cases is below 0.01%, the $\gamma = 1\%$, the $\gamma_i^{min} = 80\%$, and the Extreme Spot prices are used. Objective Value represents the optimal operational cost of step 2. Power * corresponds to the optimal power from step 1 required by the WSS to meet their demand. For the BEA model, we used N=3 partitions in all the cases. Note that Summer and Spring are abbreviated as Sum and Spri, respectively, and the PPA Average and Quarter, as Avg and Qtr.

Model	Case	Time	Obj. Val.	Power *	Power DR
SL	Sum Avg	34.4 s	$33,340	1,450 MW	166 MW
BEA	Sum Avg	1.3 s	$33,109	1,450 MW	149 MW
SL	Sum Qtr	10 min	$31,618	1,431 MW	210 MW
BEA	Sum Qtr	4.6 s	$31,373	1,431 MW	210 MW
SL	Spri Qtr	15 min	Infeasible	Infeasible	Infeasible
BEA	Spri Qtr	1.1 s	$31,904	1,420 MW	246 MW

We performed different experiments using the binary expansion approach (N=3 for the RT WSS) with Gurobi MILP, which reduces the computational time of the original MINLP while keeping the Gurobi Gap within 0.01%. Also, the BEA model slightly reduces the optimal value because it is an approximation of the original problem.

It is worth mentioning that solving this problem with Ipopt, a free non-linear solver, is not possible due to the mixed integer nature of this problem, which it doesn't support. Also, it only ensures global optimality for convex problems, and this is non-convex. Hence, we decided to use the Gurobi solver to get global optimum results in a reasonable time [3].

We included the optimal power required in a day because it is a good indicator of the solution's quality. Note that the power needed changes according to the PPA prices and the hourly temperature, which affects the water pump efficiency. In all the tested cases, the BEA model runs faster than the SL model.

6.6 Demand response provided compared to the PPA average and spot prices in summer

A WSS operator is looking to reduce its costs by pumping the demanded water in times when the PPA prices are low, and by offering DR to the power system when the gap between the Spot price and the PPA is positive. In Figure 7, we have an example of how the optimal power and the optimal DR curves move according to the PPA Average and kmeans spot prices in summer.

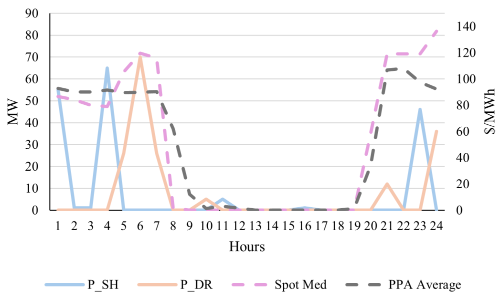

(a) P_{DR} and P_{SH} power curves with PPA Average and kmeans Price

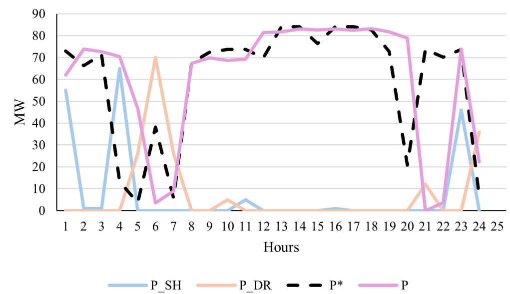

(b) Power curves in the Demand Response process

Figure 7: Example of the DR curves from step 2 compared to the optimal power operation of step 1, using the PPA Average Price and the Extreme and kmeans Spot Prices in Summer.

In Figure 7a we can see how the optimal power for DR (blue curve) and the recovery power (orange curve) interact according to the spot (magenta curve) and PPA prices (grey curve): when the gap is positive, the DR provision tends to increase, otherwise, the recovery does it. Furthermore, in Figure 7b, we can see the optimal power given by the step 1 model (black curve) and how the new power curve in magenta varies when the is DR offered (orange curve) and when there is a power recovery (blue curve).

As expected, most of the DR scheduling occurs during the early morning, evening, and night. This is because the gap between the spot price and the PPA average is positive, providing an opportunity to offer DR. Additionally, we would expect that most of the power recovery (SH) would happen during the late morning and afternoon. However, the tanks and reservoir capacity might not be sufficient to allow for this, and water demand slightly increases during this time, assuming evaporation, which puts stress on water storage. Consequently, most of the power exchange occurs during the darkest hours of the day.

6.7 PPA and spot prices comparison per season

From the results presented in Figures 8, we can see that winter has the highest operational cost in all the PPA and spot prices; however, it is the season with the highest potential to provide DR to the power system due to the WSS operator incentive of trying to reduce the operational cost as much as possible. Also, the extreme spot prices produce the biggest gap between the optimal operation cost of step 1 and step 2 compared to the kmeans spot price due to its optimistic results of the equal weights and the maximum spot price, which creates a big difference with all the PPA prices during the night and early morning.

On the other hand, the kmeans spot prices generate a more realistic expected value of the possible uncertain spot prices because they do not select extreme cases that cause the operational cost to drop sharply; instead, the centroid of each cluster is chosen, which represents a moderate price. Although this leads to lower operational cost reductions, the expected values are more lifelike than those from extreme spot prices.

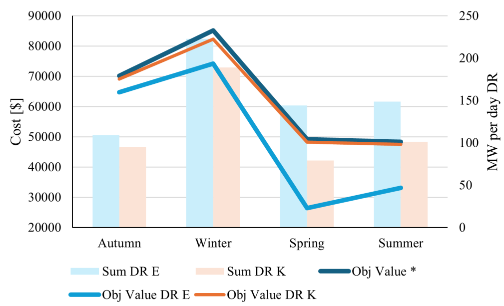

(a) PPA Average with Extreme and kmeans Spot Prices

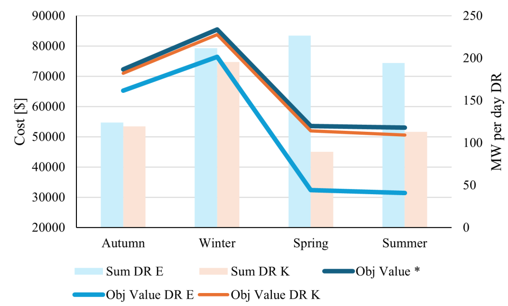

(b) PPA CNE with Extreme and kmeans Spot Prices

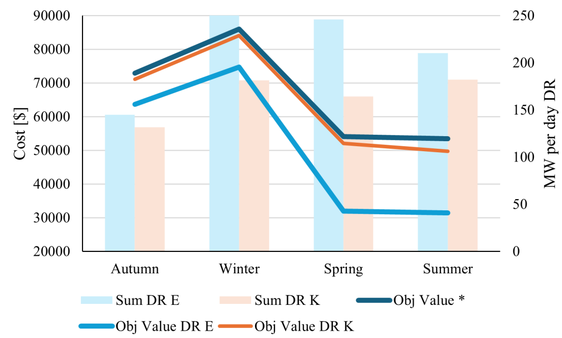

(c) PPA Quarter with Extreme and kmeans Spot Prices

Figure 8: Comparison of the different PPA per season for the Extreme and kmeans Spot Prices. The navy blue line represents the optimal step 1 cost; the light blue and orange lines represent the expected optimal cost with DR of step 2 of the Extreme and kmeans spot prices, respectively; and the light blue and orange bars show the expected number of MW the step 2 can provide of the Extreme and kmeans spot prices. Note that the E and K letters on the plots represent the Extreme and kmeans spot prices.

The PPA average and PPA CNE exhibit similar patterns and amounts of total DR provision for the kmeans spot prices, as shown in Figure 8, and confirmed by the summary presented in Table 4, with 52.9 GW and 47.1 GW, respectively. On the other hand, the PPA Quarter has a more stable pattern for DR provision, with a slightly higher amount of 60.1 GW. This means that although the PPA Quarter has a higher operational cost than the other PPAs, if the power system operator offers a bonus sufficient to cover the difference with the PPA with the best performance to the WSS operator —\$0.33M per year in this case which is offered by the PPA average— then it could potentially increase its DR reserves by 7.2 GW per year.

Table 4: Annual operational cost, cost reductions when providing DR, its relative reduction percentage, and the total DR provision for each PPA price. Results were calculated by averaging the seasons and multiplying it by 365 days for the Extreme and kmeans spot prices.

Extreme	Step 1 Cost	Cost reduct.	% reduct.	Sum DR
Average	\$23.07M	\$4.97M	21.52%	57.0 GW
CNE	\$24.11M	\$5.38M	22.30%	69.0 GW
Quarter	\$24.30M	\$5.90M	24.30%	78.3 GW
kmeans	Step 1 Cost	Cost reduct.	% reduct.	Sum DR
Average	**\$23.07M**	**\$0.52M**	**2.27%**	**52.9 GW**
CNE	\$24.11M	\$0.64M	2.67%	47.1 GW
Quarter	**\$24.30M**	**\$0.85M**	**3.52%**	**60.1 GW**

Also, by looking at Figure 9, since the medium price weight is less than a third in the kmeans case, unlike in the extreme spot price case, which has an equal weight, the objective value of the medium scenario (light blue curve) always has a lower cost in the kmeans. This is because the maximum spot price in the extreme case is very high compared to the kmeans case; therefore, the expected cost (orange curve) is lower than in the kmeans case.

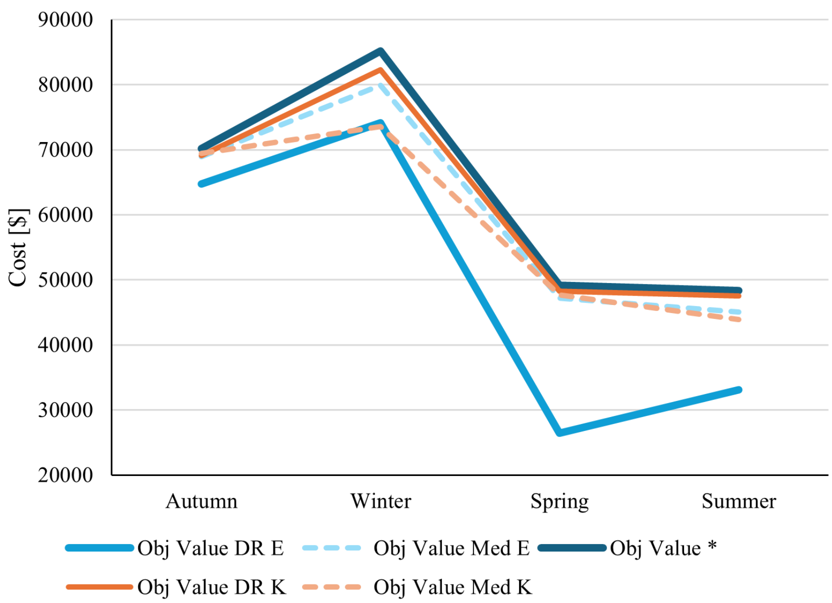

Figure 9: Comparison of the Spot prices using the PPA Average. In blue and orange tones, winter and summer are represented. The navy blue line represents the optimal step 1 cost; the light blue and orange lines represent the expected optimal cost with DR of step 2 of the Extreme and kmeans spot prices, respectively; the light blue and orange dotted lines represent the medium optimal cost with DR of step 2 of the Extreme and kmeans spot prices, respectively. Note that the E and K letters on the plots represent the Extreme and kmeans spot prices.

This confirms what we discussed in the clustering Section 6.3. By looking at the weights in Figure 5, the minimum cluster has around 60% of the total share, and the medium has around 25%, depending on the season. This results in a higher spot price for the medium case in the kmeans compared to the extreme values. Thus, not only does the medium curve remain between the optimal cost of step 1 and the expected cost in step 2 for the kmeans case, but it is also lower than the medium curve for the extreme values.

6.8 PPA comparison in summer and winter

From the point of view of the WSS operator, it would be convenient to know the best PPA price to set with the generator company. In Figure 10, we present the optimal operational cost reduction for winter and summer using the proposed PPA and kmeans spot price. This means that the higher the cost reduction, the more convenient the corresponding PPA price should be for the WSS operator. As we have discussed before, as a general rule, the PPA Average price yields lower operational costs in both seasons or the highest cost reduction; this occurs because of the flexible hourly structure, in comparison to the three and four-time blocks the CNE and Quarter PPAs offer, respectively. This can be confirmed by looking at Table 5, which shows the optimal costs of the DR model for each PPA.

Table 5: Comparison of the objective values of the step 2 for the different PPAs, kmeans spot price and for winter and summer.

	PPA Average	PPA CNE	PPA Quarter
Winter	$82,301	$83,704	$84,026
Summer	$47,485	$50,580	$49,739

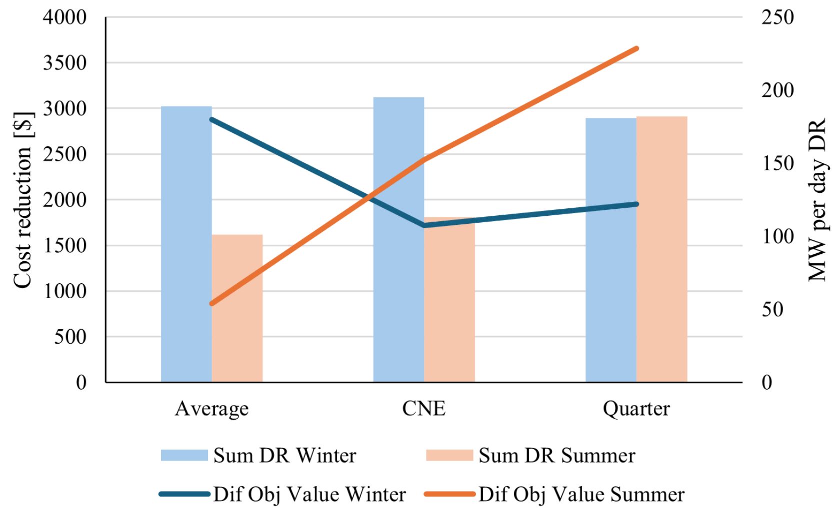

Figure 10: Comparison of the PPA Prices using the kmeans Spot Prices in Winter and Summer. In blue and orange tones, winter and summer are represented. The difference between the optimal step 1 cost and the expected optimal is illustrated by the lines, while the bars represent the expected number of MW that step 2 can provide.

Furthermore, even though the PPA average tends to have a lower price, it doesn't allow as much arbitrage to provide DR as the other PPAs, with the exception of winter, resulting in a lower flexibility range. Also, as we suspected in the previous section, the PPA Quarter seems to offer a more constant DR provision for both seasons. This, however, as we have proposed before, opens up a possibility for energy policymakers to offer bonuses for being available to provide DR in the capacity market in exchange for using other PPAs, like the Quarter one, that allow the WSSs to provide more DR. In that scenario, the WSS operators would not only be able to reduce their operational costs but also offer more DR to the power system.

6.9 Impact of the γ_d in the water demand profile in summer and winter

As we explained at the beginning of this chapter, $\gamma_d = (\sum_{t \in T} q_M \gamma)^2$ is one of the main parameters in the step 1 model, which determines how much the water demand Δd can deviate. For the purpose of this study, we decided to analyse the impact of different γ values in the DR provision. We selected the following range for $\gamma = [0.50\%, 0.75\%, 1.00\%, 1.25\%, 1.50\%]$ and examined its effects in winter and summer for the different PPAs and Spot prices. Note that the bigger the γ is, the lower the water demand tends to be.

As expected, the cost reduction increases when the water demand profile drops in Winter and Summer for all the PPA prices, as we can see in Figures 11. At the same time, the DR provided growths because there is more flexibility to use the water tank and reservoirs. This feature can be used as an advantage in months or days when the expected water demand is lower; therefore, depending on the PPA price and the possible bonus for being available to provide the DR service to the power system, WSS operators can leverage this opportunity to reduce even more their costs.

An interesting case happens in winter because the cost reduction slightly increases for all the PPA prices, and so does the total possible DR provision. Also, the total provision doubles the one in summer in all the PPA prices, except for the PPA Quarter, which remains almost stable throughout the seasons, as we talked about earlier. For summer, the PPA with the biggest relative cost reduction is the PPA Quarter, followed by the PPA CNE and the PPA Average; nevertheless, the PPA Average is the one with the lowest mean operational cost, as we can see in Table 6.

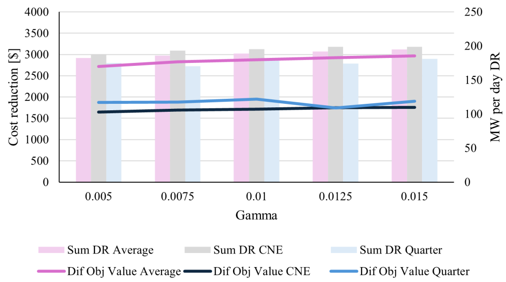

(a) Different γ_d in Winter

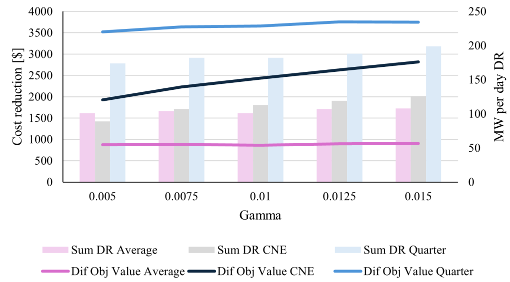

(b) Different γ_d in Summer

Figure 11: Comparison of the PPA Quarter per season for the Extreme and kmeans Spot Prices. In navy blue, the optimal step 1 cost is displayed; in orange, the expected optimal cost with DR of step 2 is shown; in light blue, the optimal cost for the medium spot price of step 2 is displayed; and the grey bars represent the expected number of MW the step 2 can provide.

Table 6: Average of the daily operational costs after providing DR of all the γ_d tested for Winter and Summer with kmeans spot price.

	PPA Average	PPA CNE	PPA Quarter
Winter	\$82,318	\$83,708	\$84,113
Summer	\$47,484	\$50,610	\$49,740

6.10 Impact of the minimum power to provide DR

As mentioned in the introduction, the Chilean power system is still evolving, and different policies regarding DR provision are being analysed. In this context, we aimed to explore how the flexibility opportunities for WSS increase or decrease under different minimum power requirements for providing DR to the power systems. This study can help not only WSS operators decide whether to enter DR schemes but also provide insights to energy policymakers on how to define DR schemes based on industry needs and possibly the region of the country.

Consequently, for this section, we analysed the impact of the minimum power needed by energy consumers to provide DR to the system. We tested the following values for $P^{DR}_{min} = [0.5, 1.0, 3.0, 5.0, 7.0, 10.0]$ MW, using the PPA Average, the kmeans spot prices, and the Winter and Summer time.

In Figure 12 we observe the optimal DR provision for the day, the cost reduction achieved by offering DR compared to the step 1 operational model, and the number of hours in a day that the WSS has committed to delivering DR to the power system. As discussed in the prior sections, winter offers the greatest cost reduction and DR provision compared to summer, with around 100 MW more per day. Unlike summer, winter benefits from a lower minimum power requirement for DR from both the WSS operator's and the power system's perspectives. This is because the tendency for power delivered and cost slightly decreases when the minimum power grows, as shown in Figure 12a.

Conversely, during summer, power systems benefit from a larger minimum power for DR due to an increase in the total DR provided per day, while the WSS lowers its operational cost reduction. Therefore, an alternative for power systems to have more flexibility available during summer is to set a larger minimum DR power but offer a bigger bonus to clients to compensate for the opportunity cost of increased operational cost reduction.

As expected, when the minimum DR power increases, the number of DR activations, i.e., the number of hours the DR service is provided by the WSS, decreases, as seen in Figure 12b. This is because the WSS consumes around 60 MW on average, and thus, the 10 MW minimum requirement represents a sixth of its total hourly need. Hence, with a lower P^{DR}_{min}, the WSS is more likely to offer DR more frequently throughout the day. Additionally, since the WSS can provide DR during more hours in the day, it is more advantageous in winter as it can leverage the gap between the spot and PPA prices for its operational cost, making good use of the spot price variability.

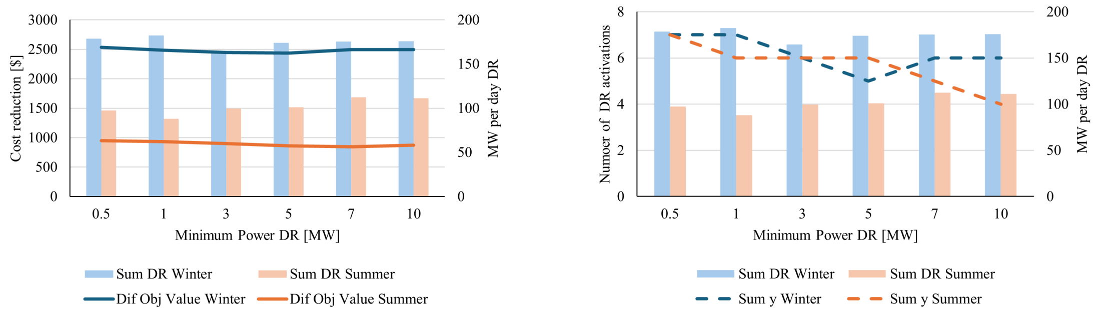

(a) Different P_{min}^{DR} values - Cost vs DR provision

(b) Different P_{min}^{DR} values - Number DR activations vs DR provision

Figure 12: Comparison of the minimum power to provide DR using the kmeans Spot Prices and the PPA Average. In blue tones, the winter values are shown, and in orange tones, the summer time values. The difference between the optimal step 1 cost and the expected optimal can be seen in the lines on the left plot, and the bars represent the expected number of MW that step 2 can provide. On the right plot, the lines represent the number of hours the DR scheduling is activated, i.e. the variable y_t.

6.11 Impact on DR of the minimum water level in resevoirs

As formerly explained, some industries require a minimum level in their water reservoirs due to the high inelasticity of this resource, where the unavailability of water can result in multimillion-dollar losses. For instance, the copper mine CODELCO aims to maintain their reservoirs between 90-95% [3]. Therefore, the final study in this work examines the effect of the reservoir minimum level set at 50%, 80%, and 90%, using the PPA average and the kmeans spot price.

As we can see in Figure 13, the cost reduction grows when the minimum reservoir level is lowered. Generally, the lower the minimum reservoir level, the more DR the WSS can provide. This effect is particularly noticeable in winter when the difference between the 50% and 90% levels is nearly 50 MW per day. Additionally, the most significant drop in cost reduction occurs between the 80% and 90% curves, indicating that WSS can reduce operational costs by almost \$3,000 per day in winter if they lower their minimum level from 90-95% to 80%. However, the cost reduction from the 80% to the 50% reservoir minimum level is not significant and ultimately depends on the WSS operator's willingness to assume the associated risk for the stored water. The total annual cost reduction is \$0.55M (2.46%), \$0.52M (2.27%), and \$0.48M (2.08%) for the 50%, 80%, and 90% reservoir minimum levels, respectively; and the yearly DR provision would be around 44.6 GW, 42.3 GW and 41.7 GW, for each case.

Finally, if the WSS operator is willing to reduce the minimum reservoir level during operation, and policymakers introduce a bonus for being available to provide DR, an alternative optimal scenario arises. This scenario results in operational cost reduction for the WSS and maximises DR provision for the power system.

6.12 Simulator analysis results

A simulator was built to check the quality of the solutions of power profile optimisation with the DR model in step 2. For this purpose, we used the fixed water profile from step 1: optimal power P^* and the optimal water demand profile $d^* + \Delta d^*$, and the fixed optimal power shift schedule from step 2: optimal water pump scheduling x^* and optimal DR schedule y^*. With these fixed parameters, we solved the step 2 model with a single scenario: simulated spot price per season.

For the simulated spot prices, we took all the days in one season and created new instances using a deviation band of 10%, resulting in 1000 spot prices.

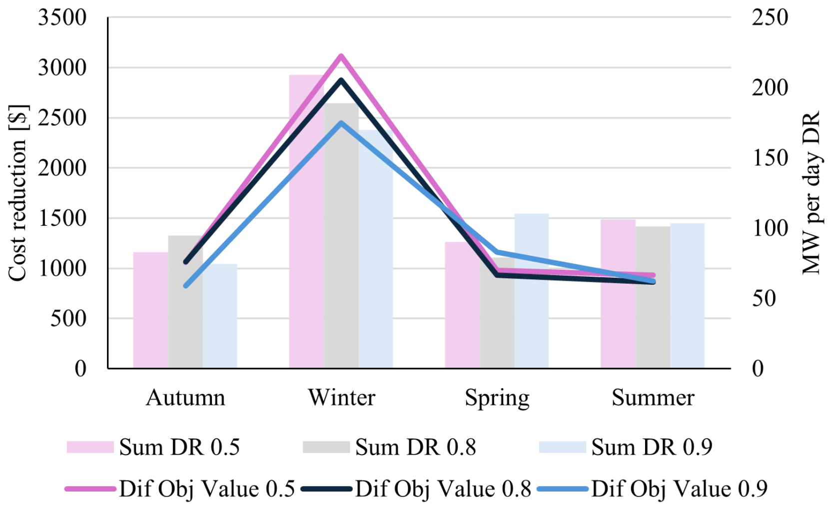

Figure 13: Comparison of the reservoir minimum level using the proposed kmeans Spot Price and the PPA Average is shown. The 50% reservoir minimum level is depicted in magenta tones, the 80% reservoir minimum level in black tones, and the 90% reservoir minimum level in blue tones. The difference between the optimal step 1 cost and the expected optimal is illustrated by the lines, while the bars represent the expected number of MW that step 2 can provide.

In Table 7, we can see the optimal operational cost from the step 1 model, compared to the average result of all the simulated independent runs using the 1000 scenarios of model 2 with the optimal scheduling solutions from step 2 with kmeans spot prices. We can conclude that, on average, providing demand response reduces between $1000 to $5000 per day. Also, all the simulations resulted in feasible solutions. We can see that summer has a better chance of ending up with a lower operational cost than winter, as shown in the last column of the table.

Table 7: Results for the validation model of the simulation analysis. The optimal operational cost of step 1, the average operational cost of all the simulations using the step 2 model, and the percentage of cases that have lower total costs compared to the step 1 solution are shown in this table.

Case	Obj Value *	Mean Obj Value DR	Cases with Lower Cost DR
Win Avg	$82,300	$79,428	**51%**
Win CNE	$83,703	$81,197	47%
Win Qtr	$84,026	$80,758	28%
Sum Avg	$47,484	$46,777	40%
Sum CNE	$50,580	$45,837	**63%**
Sum Qtr	$49,738	$44,589	**69%**

In summary, the BEA technique allows us to solve the optimal operation of a water network in a reasonable computational time with a small gap. The latter is relevant because the WSS operator needs to have a solution on a day-ahead basis to determine the DR bidding scheme for the next day. Also, the DR model for the WSS operation reduces the total cost while delivering DR to the power system without compromising the water supply. Furthermore, the PPA Average offers the best operational costs but one of the lower DR provisions to the power system, unlike the PPA Quarter, however, since the latter has a lower operational costs reduction, the possibility to create a bonus for being available in the capacity market, and allow a reduction in the electrical demand appears as an attractive alternative for both the WSS and power system operators, depending on the season and minimum DR power requirement.

7 Conclusion and future research

This paper presents a new two-step stochastic model for water pump scheduling problems with demand response (DR), accounting for uncertain water demand and electricity prices, which was solved using the binary expansion approach. The problem aims to minimise energy costs in large-scale multi-tank and high-altitude WSS while providing demand response to the power network. The method was tested with real-life water supply systems (WSS) from the Radomiro Tomic Mine in Chile, and different policies for both the WSS and electricity operator were proposed. The critical findings obtained are as follows:

1. **WSS are promising candidates to provide DR to the power network** due to the price arbitrage between the spot prices and the PPA price contracts, as we proved in this paper. In particular, the Chilean copper mine Radomiro Tomic's WSS could potentially offer between 47 GW and 60 GW a year of DR and reduce its annual operational costs between \$0.52M and \$0.82, depending on the PPA price. This allows the electrical bus from that place to have that amount of demand flexibility and, therefore, to continue with the efforts of introducing more renewable generation to the power system.
2. The binary expansion approach performs better than the MINLP Gurobi solver for the demand response model. The computational efficiency of the approach gives the chance to use it for hours or for day-ahead operation, such as many types of electrical demand flexibility models in big WSS. In particular, the speed of the approach allows the calculation of an accurate expected value for the total operational costs under many spot price scenarios.
3. The **influence of temperature** across various months significantly affects the overall expenses of WSS operations: the warmer the month, the cheaper the electrical tariffs become due to an excess of solar generation, leading to reduced operational costs as well. However, in seasons when the temperature is outside of the pump efficiency range, the water pumping process becomes more energy expensive.
4. The PPA contracts, although unknown for the purpose of this work, have a great impact on the operation cost, the DR benefits and the amount of DR that can be provided by the WSSs. However, the more flexible the PPA prices are, the better the chances to reduce the costs and offer more DR to the power system. In that sense, from the point of view of the WSS operator, PPA prices that are similar to the **PPA Average** calculated in this research give the best outcome for reducing operational costs.
5. Winter offers the greatest potential for DR due to the incentives to reduce the operational costs of WSSs. The gap between the original operational model and the model with DR could widen further if additional incentives are provided by the electrical coordinator, such as a payment for being available to provide DR in the capacity market, in addition for the compensation for differences in PPA prices. Such payments would further incentivise WSS operators to offer demand flexibility.
6. The increase in the water demand slightly increases the operational cost for all the PPA prices for both summer and winter. Also, the PPA Average offers the lowest cost reduction in summer but the highest in winter, which shows the potential for cost reduction in the wintertime.
7. The change in the **minimum power requirement** offers the possibility of a different energy policy for winter and summer. Winter benefits from a lower minimum power requirement for DR from both the WSS operator and the power system's perspectives. In summer, the power systems benefit from a larger minimum power for DR due to an increase in the total DR provided per day, while the WSS lowers its operational cost reduction. Therefore, an alternative for power systems to have more flexibility available during summer is to set a larger minimum DR power but offer a bigger bonus to clients to compensate for the opportunity cost of increased operational cost reduction.

8. The operational strategy of having a minimum level of water in reservoirs of 80% or 50% yields minimal changes in costs; however, going from a **reservoir minimum water level from 90 to 80% produces the most significant cost reduction**. Therefore, the cost reduction and water risk level trade-off is left to the WSS operator. Also, maintaining a lower level increases the DR provision throughout the day, which allows a space to provide more flexibility to the electrical grid.
9. **Energy policymakers could offer bonuses to WSS operators for being available to provide DR** to the power system. In this scenario, WSS would reduce its operational costs and increase its DR contribution to the capacity market. This would encourage energy-intensive infrastructures, such as WSSs, to participate in the capacity market by providing the right incentives and tools. The power system would gain additional sources of demand flexibility, which is crucial for the reliable integration of renewable generation sources.

Finally, the DR model for WSS proposed in this paper can be used to further extend the problem; in particular, we propose the following lines of research. We suggest using representative days or months for the temperature instead of the seasons to gain a better understanding of the weather and its impact on the amount of DR that can be provided. Additionally, using representative days for electricity prices would help propose a better PPA price contract and improve spot price forecasts. Also, including the different electrical buses connected to specific nodes in the WSS in the model will allow for a more precise representation of reality. Furthermore, other factors, such as CO_2 emissions, the use of fixed-speed water pumps, and the possibility of blackouts in the power system, should be analysed to ensure the WSS can operate reliably. Further, metrics like the Conditional Value at Risk (CVar), with its corresponding spot price distribution and forecast, should be used to understand the impact on the expected objective value, considering the risk of being unable to reduce operational costs with the DR model. Lastly, further analysis could explore other industries related to WSS, such as agriculture and residential areas, which may present non-directed and cyclical graphs and involve multiple operators. In these cases, both non-centralised water operators and energy market players should be considered. Future work in this area will deepen our understanding of WSS's role in the demand flexibility market and how energy policymakers can motivate their participation in the capacity market. The ultimate goal is to facilitate a quicker, safer, and more reliable integration of renewable generation sources.

Appendix A Tables

Table A1: Data of the nodes of the RT WSS [3].

Node	Altitude	Node Type	Area tank	Height tank	Start/final storage	Demand
1	30 m	RO	-	-	-	-2.0
2	30 m	Tank	800 m^2	10 m	50%	-
3	1,100 m	Junction	-	-	-	-
4	1,100 m	Tank	800 m^2	10 m	50%	-
5	1,600 m	Junction	-	-	-	-
6	1,600 m	Tank	800 m^2	10 m	50%	-
7	2,100 m	Junction	-	-	-	-
8	2,100 m	Tank	800 m^2	10 m	50%	-
9	2,600 m	Junction	-	-	-	-
10	2,600 m	Tank	800 m^2	10 m	50%	-
11	3,100 m	Junction	-	-	-	-
12	3,100 m	Reservoir	1,000 m^2	16 m	90%	-
13	3,100 m	Mine	-	-	-	1.5

Table A2: Data of the arcs of the RT WSS [3].

Node i	Node j	Arc Type	Length [m]
1	2	Pipe	1
2	3	Pump	30
3	4	Pipe	6,300
4	5	Pump	-
5	6	Pipe	85,000
6	7	Pump	-
7	8	Pipe	21,800
8	9	Pump	-
9	10	Pipe	22,500
10	11	Pump	-
11	12	Pipe	17,400
12	13	Pipe	1

Table A3: Daily temperature in Calama in 2023-2024 per season. The temperature in bold represents the hours when the temperature is out of bounds of the optimal water pump efficiency range. Data taken from [82].

Hour	Jul [°C]	Oct [°C]	Jan [°C]	Mar [°C]
1	**4**	10	16	9
2	**3**	8	14	9
3	**1**	7	12	9
4	**4**	8	11	8
5	**5**	**5**	10	8
6	8	8	10	7
7	7	**5**	10	6
8	7	6	11	**5**
9	10	13	16	15
10	15	18	20	15
11	18	21	22	18
12	20	22	**24**	21
13	21	23	**25**	22
14	21	**24**	**26**	22
15	21	**24**	**26**	22
16	22	**25**	**26**	23
17	20	**25**	**26**	22
18	19	**25**	**26**	22
19	15	23	**26**	20
20	11	21	**24**	19
21	10	17	21	17
22	**4**	15	19	15
23	**5**	14	19	13
24	**5**	11	17	10
Mean	11.5	15.8	19.0	14.9

Table A4: Water density values between 0 °C and 100 °C [64, 65].

T [°C]	ρ [kg/m^3]	T [°C]	ρ [kg/m^3]	T [°C]	ρ [kg/m^3]
0 (ice)	917.00	33	994.76	67	979.34
0	999.82	34	994.43	68	978.78
1	999.89	35	994.08	69	978.21
2	999.94	36	993.73	70	977.63
3	999.98	37	993.37	71	977.05
4	1000.00	38	993.00	72	976.47
5	1000.00	39	992.63	73	975.88
6	999.99	40	992.25	74	975.28
7	999.96	41	991.86	75	974.68
8	999.91	42	991.46	76	974.08
9	999.85	43	991.05	77	973.46
10	999.77	44	990.64	78	972.85
11	999.68	45	990.22	79	972.23
12	999.58	46	989.80	80	971.60
13	999.46	47	989.36	81	970.97
14	999.33	48	988.92	82	970.33
15	999.19	49	988.47	83	969.69
16	999.03	50	988.02	84	969.04
17	998.86	51	987.56	85	968.39
18	998.68	52	987.09	86	967.73
19	998.49	53	986.62	87	967.07
20	998.29	54	986.14	88	966.41
21	998.08	55	985.65	89	965.74
22	997.86	56	985.16	90	965.06
23	997.62	57	984.66	91	964.38
24	997.38	58	984.16	92	963.70
25	997.13	59	983.64	93	963.01
26	996.86	60	983.13	94	962.31
27	996.59	61	982.60	95	961.62
28	996.31	62	982.07	96	960.91
29	996.02	63	981.54	97	960.20
30	995.71	64	981.00	98	959.49
31	995.41	65	980.45	99	958.78
32	995.09	66	979.90	100	958.05

References

[1] B. Coelho, A. Andrade-Campos, Efficiency achievement in water supply systems - A review, Renewable and Sustainable Energy Reviews 30 (2014) 59–84. doi:10.1016/j.rser.2013.09.010.

[2] C. Mkireb, A. Dembélé, A. Jouglet, T. Denoeux, Robust Optimization of Demand Response Power Bids for Drinking Water Systems, Applied Energy 238 (2019) 1036–1047. doi:10.1016/J.APENERGY.2019.01.124.

[3] D. Cariaga, A. Lorca, M. F. Anjos, A Binary Expansion Approach for the Water Pump Scheduling Problem in Large and High-Altitude Water Supply Systems, Energies 17 (2024). URL: https://www.mdpi.com/1996-1073/17/16/4107. doi:10.3390/en17164107.

[4] M. Arellano Hernandez, Estudio de las variables que influyen en la escasez hídrica en la zona Norte de Chile y análisis crítico de los planes existentes., Ph.D. thesis, University of Chile, 2021.

[5] Government of Chile, Ministro de Energía anuncia que "para el 2025 habremos retirado el 50% de las centrales a carbón"., 2021. URL: https://www.gob.cl/noticias/ministro-de-energia-anuncia-que-para-el-2025-habremos-retirado-el-50-de-las-centrales-a-carbon/.

[6] Generadoras de Chile, Generación Eléctrica en Chile, 2024. URL: https://generadoras.cl/generacion-electrica-en-chile.

[7] Ministerio de Energía de Chile, POLÍTICA ENERGÉTICA NACIONAL, Technical Report, 2022. URL: https://www.chileagenda2030.gob.cl/iniciativas/1985/documento/pen_2050_-_actualizado_marzo_2022_0.pdf.

[8] H. Chandler, Empowering Variable Renewables - Options for Flexible Electricity Systems, Technical Report, IEA, 2008.

[9] S. Impram, S. Varbak Nese, B. Oral, Challenges of renewable energy penetration on power system flexibility: A survey, Energy Strategy Reviews 31 (2020) 100539. URL: https://doi.org/10.1016/j.esr.2020.100539. doi:10.1016/j.esr.2020.100539.

[10] J. Cochran, M. Miller, O. Zinaman, M. Milligan, D. Arent, B. Palmintier, M. O'Malley, S. Mueller, E. Lannoye, A. Tuohy, B. Kujala, M. Sommer, H. Holttinen, J. Kiviluoma, S. K. Soonee, Flexibility in 21st Century Power Systems (2014). URL: http://www.osti.gov/scitech/biblio/1130630. doi:10.2172/1130630.

[11] U S Department of Energy, Benefits of Demand Response in Electricity Markets and Recommendations for Achieving Them, U.S. Department of Energy (2006) 122.

[12] M. H. Albadi, E. F. El-Saadany, A summary of demand response in electricity markets, Electric Power Systems Research 78 (2008) 1989–1996. doi:10.1016/j.epsr.2008.04.002.

[13] F. Mohammadi, M. Sahraei-ardakani, Y. Al-abdullah, Coordinated Operation of Power Generation and Water Desalination, IFAC-PapersOnLine 51 (2018) 456–461. URL: https://doi.org/10.1016/j.ifacol.2018.11.745. doi:10.1016/j.ifacol.2018.11.745.

[14] H. Meschede, Increased utilisation of renewable energies through demand response in the water supply sector – A case study, Energy 175 (2019) 810–817. URL: https://doi.org/10.1016/j.energy.2019.03.137. doi:10.1016/j.energy.2019.03.137.

[15] K. Oikonomou, M. Parvania, Optimal Coordinated Operation of Interdependent Power and Water Distribution Systems, IEEE Transactions on Smart Grid 11 (2020) 4784–4794. doi:10.1109/TSG.2020.3000173.

[16] M. Pied, M. F. Anjos, R. P. Malhamé, A flexibility product for electric water heater aggregators on electricity markets, Applied Energy 280 (2020) 115168. URL: https://doi.org/10.1016/j.apenergy.2020.115168. doi:10.1016/j.apenergy.2020.115168.

[17] S. Sichilalu, X. Xia, J. Zhang, Optimal scheduling strategy for a grid-connected photovoltaic system for heat pump water heaters, Energy Procedia 61 (2014) 1511–1514. URL: http://dx.doi.org/10.1016/j.egypro.2014.12.158. doi:10.1016/j.egypro.2014.12.158.

[18] R. Menke, E. Abraham, P. Parpas, I. Stoianov, Demonstrating demand response from water distribution system through pump scheduling, Applied Energy 170 (2018). doi:10.1016/j.apenergy.2016.02.136.

[19] K. Oikonomou, M. Parvania, R. Khatami, Optimal Demand Response Scheduling for Water Distribution Systems, IEEE Transactions on Industrial Informatics 14 (2018). doi:10.1109/TII.2018.2801334.

[20] A. Stuhlmacher, L. A. Roald, J. L. Mathieu, Tractable Robust Drinking Water Pumping to Provide Power Network Voltage Support, Proceedings of the IEEE Conference on Decision and Control 2021-Decem (2021) 4206–4213. doi:10.1109/CDC45484.2021.9683419.

[21] R. Smith, K. Meng, Z. Dong, Demand response : a strategy to address residential air-conditioning peak load in Australia 1 (2013) 223–230. doi:10.1007/s40565-013-0032-0.

[22] S. Nan, M. Zhou, G. Li, Optimal residential community demand response scheduling in smart grid, Applied Energy 210 (2018). doi:10.1016/j.apenergy.2017.06.066.

[23] M. Salgado, M. Negrete-Pincetic, A. Lorca, D. Olivares, A low-complexity decision model for home energy management systems, Applied Energy 294 (2021) 116985. URL: https://doi.org/10.1016/j.apenergy.2021.116985. doi:10.1016/j.apenergy.2021.116985.

[24] B. Sparn, R. Hunsberger, Opportunities and Challenges for Water and Wastewater Industries to Provide Exchangeable Services, National Renewable Energy Laboratory (NREL) (2015) Water Scarcity and Climate Change Enabling Environ. URL: https://www.nrel.gov/docs/fy16osti/63931.pdf.

[25] R. D. Garreaud, J. P. Boisier, R. Rondanelli, A. Montecinos, H. H. S. D. Veloso-Aguila, The Central Chile Mega Drought (2010 – 2018): A climate dynamics perspective, International Journal of Climatology 40 (2020) 421–439. doi:10.1002/joc.6219.

[26] S. Vicuña, M. Gil, O. Melo, G. Donoso, P. Merino, S. Vicuña, M. Gil, O. Melo, G. Donoso, P. Merino, M. Gil, Water option contracts for climate change adaptation in Santiago , Chile, Water International 43 (2018) 237–256. URL: https://doi.org/10.1080/02508060.2017.1416444. doi:10.1080/02508060.2017.1416444.

[27] S. Herrera, L. A. Cisternas, E. D. Gálvez, Simultaneous Design of Desalination Plants and Distribution Water Network, in: Computer Aided Chemical Engineering, volume 37, 2015. doi:10.1016/B978-0-444-63577-8.50044-9.

[28] COCHILCO, Agua en la minería del Cobre (2023) 1–37.

[29] COCHILCO, Water demand projections in the copper mining industry (2023). URL: https://www.cochilco.cl/ListadoTemtico/Proyeccindedemandadeaguaenlamineradelcobre.pdf.

[30] COCHILCO, Proyección del consumo de energía eléctrica en la minería del cobre 2022-2033 (2023).

[31] L.-B. De la perrière, A. Jouglet, D. Nace, Optimisation de la gestion des réseaux d'eau potable par la programmation linéaire en nombre entiers., Ph.D. thesis, Université de Technologie de Compiègne, 2011.

[32] C. D'Ambrosio, A. Lodi, S. Wiese, C. Bragalli, Mathematical programming techniques in water network optimization, European Journal of Operational Research 243 (2015) 774–788. doi:10.1016/j.ejor.2014.12.039.

[33] M. Abdallah, Z. Kapelan, Fast Pump Scheduling Method for Optimum Energy Cost and Water Quality in Water Distribution Networks with Fixed and Variable Speed Pumps, Journal of Water Resources Planning and Management 145 (2019) 1–13. doi:10.1061/(asce)wr.1943-5452.0001123.

[34] A. M. Bagirov, A. F. Barton, H. Mala-Jetmarova, A. Al Nuaimat, S. T. Ahmed, N. Sultanova, J. Yearwood, An algorithm for minimization of pumping costs in water distribution systems using a novel approach to pump scheduling, Mathematical and Computer Modelling 57 (2013) 873–886. URL: http://dx.doi.org/10.1016/j.mcm.2012.09.015. doi:10.1016/j.mcm.2012.09.015.

[35] M. López-ibáñez, T. D. Prasad, B. Paechter, Ant Colony Optimization for Optimal Control of Pumps in Water Distribution Networks 134 (2008) 337–346. doi:10.1061/(ASCE)0733-9496(2008)134.

[36] B. Ulanicki, J. Kahler, H. See, Dynamic Optimization Approach for Solving an Optimal Scheduling Problem in Water Distribution Systems, Journal of Water Resources Planning and Management 133 (2007) 23–32. doi:10.1061/(asce)0733-9496(2007)133:1(23).

[37] B. Coulbeck, M. Brdys, C. H. Orr, J. P. Rance, A hierarchical approach to optimized control of water distribution systems: Part II. Lower-level algorithm, Optimal Control Applications and Methods 9 (1988) 109–126. doi:https://doi.org/10.1002/oca.4660090202.

[38] B. Coulbeck, M. Brdys, C. H. Orr, J. P. Rance, A hierarchical approach to optimized control of water distribution systems: Part I decomposition, Optimal Control Applications and Methods 9 (1988) 51–61. doi:https://doi.org/10.1002/oca.4660090105.

[39] F. Fallside, P. F. Perry, Hierarchial model for water-supply-system control, Proceedings of the IEEE 122 (1975) 441–443. doi:10.1049/piee.1975.0121.

[40] M. Sterling, B. Coulbeck, Optimisation of water pumping costs by hierarchical methods, Proceedings of the Institution of Civil Engineers 59 (1975) 789–797. doi:https://doi.org/10.1680/iicep.1975.3639.

[41] E. Alperovits, U. Shamir, Design of optimal water distribution systems, Water Resources Research 13 (1977) 885–900. doi:https://doi.org/10.1029/WR013i006p00885.

[42] J. Schwarz, N. Meidad, U. Shamir, Water quality management in regional systems, Water Resources Management 153 (1985) 341–349. URL: https://pascal-francis.inist.fr/vibad/index.php?action=getRecordDetail&idt=8434836.

[43] L. E. Ormsbee, T. M. Walski, D. V. Chase, W. W. Sharp, Methodology for improving pump operation efficiency, Journal of Water Resources Planning and Management 115 (1989) 148–164. doi:10.1061/(ASCE)0733-9496(1989)115:2(148).

[44] A. Morsi, B. Geißler, A. Martin, Mixed Integer Optimization of Water Supply Networks, in: Mathematical Optimization of Water Networks. International Series of Numerical Mathematics, vol 162, Birkhäuser, Basel, 2012. URL: https://doi.org/10.1007/978-3-0348-0436-3_3.

[45] H. Mala-Jetmarova, N. Sultanova, D. Savic, Lost in optimisation of water distribution systems? A literature review of system operation, Environmental Modelling and Software 93 (2017) 209–254. URL: http://dx.doi.org/10.1016/j.envsoft.2017.02.009. doi:10.1016/j.envsoft.2017.02.009.

[46] A. Stuhlmacher, J. L. Mathieu, Chance-Constrained Water Pumping to Manage Water and Power Demand Uncertainty in Distribution Networks, Proceedings of the IEEE 108 (2020) 1640–1655. doi:10.1109/JPROC.2020.2997520.

[47] Y. Liu, C. Barrows, J. Macknick, M. Mauter, Optimization Framework to Assess the Demand Response Capacity of a Water Distribution System, Journal of Water Resources Planning and Management 146 (2020) 1–13. doi:10.1061/(asce)wr.1943-5452.0001258.

[48] K. Oikonomou, M. Parvania, Optimal Participation of Water Desalination Plants in Electricity Demand Response and Regulation Markets, IEEE Systems Journal 14 (2020) 3729–3739. doi:10.1109/JSYST.2019.2943451.

[49] A. Shapiro, D. Dentcheva, A. Ruszczyński, Lectures on Stochastic Programming, Society for Industrial and Applied Mathematics, 2009. URL: https://epubs.siam.org/doi/abs/10.1137/1.9780898718751. doi:10.1137/1.9780898718751.

[50] W. B. Powell, A unified framework for stochastic optimization, European Journal of Operational Research 275 (2019) 795–821. URL: https://doi.org/10.1016/j.ejor.2018.07.014. doi:10.1016/j.ejor.2018.07.014.

[51] T. Homem-de Mello, G. Bayraksan, Monte Carlo sampling-based methods for stochastic optimization, Surveys in Operations Research and Management Science 19 (2014) 56–85. URL: http://dx.doi.org/10.1016/j.sorms.2014.05.001. doi:10.1016/j.sorms.2014.05.001.

[52] A. Zakaria, F. B. Ismail, M. S. Lipu, M. A. Hannan, Uncertainty models for stochastic optimization in renewable energy applications, Renewable Energy 145 (2020) 1543–1571. URL: https://doi.org/10.1016/j.renene.2019.07.081. doi:10.1016/j.renene.2019.07.081.

[53] J. Burgschweiger, B. Gnädig, M. C. Steinbach, Optimization models for operative planning in drinking water networks (2009) 43–73. doi:10.1007/s11081-008-9040-8.

[54] D. Bertsimas, E. Litvinov, X. A. Sun, J. Zhao, T. Zheng, Adaptive robust optimization for the security constrained unit commitment problem, IEEE Transactions on Power Systems 28 (2013) 52–63. doi:10.1109/TPWRS.2012.2205021.

[55] S. Herrera-León, F. Lucay, A. Kraslawski, L. A. Cisternas, E. D. Gálvez, Optimization Approach to Designing Water Supply Systems in Non-Coastal Areas Suffering from Water Scarcity, Water Resources Management 32 (2018). doi:10.1007/s11269-018-1939-z.

[56] D. Fooladivanda, J. A. Taylor, Energy-optimal pump scheduling and water flow, IEEE Transactions on Control of Network Systems 5 (2018) 1016–1026. doi:10.1109/TCNS.2017.2670501.

[57] S. Herrera-León, A. Kraslawski, L. A. Cisternas, A MINLP model to design desalinated water supply systems including solar energy as an energy source, in: Computer Aided Chemical Engineering, volume 44, 2018. doi:10.1016/B978-0-444-64241-7.50276-7.

[58] C. Bragalli, C. D'Ambrosio, J. Lee, A. Lodi, P. Toth, On the optimal design of water distribution networks: A practical MINLP approach, Optimization and Engineering 13 (2012) 219–246. doi:10.1007/s11081-011-9141-7.

[59] A. Fugenschuh, J. Humpola, A Unified View on Relaxations for a Nonlinear Network Flow Problem, Technical Report July, Zuse Institut Berlin, 2013.

[60] P. Bhave, R. Gupta, Analysis of Water Distribution Networks, Oxford, U.K.: Alpha Science International, Oxford, UK, 2006.

[61] Q. Li, S. Yu, A. S. Al-Sumaiti, K. Turitsyn, Micro water-energy nexus: Optimal demand-side management and quasi-convex hull relaxation, IEEE Transactions on Control of Network Systems 6 (2019) 1313–1322. doi:10.1109/TCNS.2018.2889001.

[62] A. Kayode Coker, Pumping of liquids, in: Ludwig's Applied Process Design for Chemical and Petrochemical Plants, 2007, pp. 303–369. doi:10.1016/b978-075067766-0/50012-9.

[63] B. Stoffel, The Role of Pumps for Energy Consumption and Energy Saving, Assessing the Energy Efficiency of Pumps and Pump Units (2015) 1–24. doi:10.1016/b978-0-08-100597-2.00001-x.

[64] Water Science School, Water Density, 2018. URL: https://www.usgs.gov/special-topics/water-science-school/science/water-density.

[65] Valves Instruments Plus Ltd, Density Of Liquid Water From 0°C to 100°C, 2024. URL: https://www.vip-ltd.co.uk/Expansion/Density_Of_Water_Tables.pdf.

[66] J. E. van Zyl, D. A. Savic, G. A. Walters, Operational Optimization of Water Distribution Systems Using a Hybrid Genetic Algorithm, Journal of Water Resources Planning and Management 130 (2004) 160–170. doi:10.1061/(asce)0733-9496(2004)130:2(160).

[67] K. E. Lansey, K. Awumah, Optimal Pump Operations Considering Pump Switches, Journal of Water Resources Planning and Management 120 (1994) 17–35. doi:https://doi.org/10.1061/(ASCE)0733-9496(1994)120:1(17).

[68] D. Savic, G. Walters, M. Schwab, Multiobjective genetic algorithms for pump scheduling in water supply, Evolutionary Computing. Lecture Notes in Computer Science 1305 (1997). doi:https://doi.org/10.1007/BFb0027177.

[69] R. Menke, E. Abraham, P. Parpas, I. Stoianov, Approximation of system components for pump scheduling optimisation, in: Procedia Engineering, volume 119, 2015. doi:10.1016/j.proeng.2015.08.935.

[70] Comisión Nacional de Energía, Norma Técnica de Servicios Complementarios. CNE (2019) 111. URL: https://www.cne.cl/wp-content/uploads/2020/05/NT-SSCC.pdf.

[71] Comisión Nacional de Energía, Resolución Exenta N 442 Servicios Complementarios Chile 21 (2020) 1–9.

[72] O. Gunluk, J. Lee, J. Leung, A Polytope for a Product of Real Linear Functions in 0/1 Variables, Mixed Integer Nonlinear Programming. The IMA Volumes in Mathematics and its Applications 154 (2012) 513–529. doi:10.1007/978-1-4614-1927-3.

[73] T. Tapia, A. Lorca, D. Olivares, M. Negrete-Pincetic, A. J. Lamadrid L, A robust decision-support method based on optimization and simulation for wildfire resilience in highly renewable power systems, European Journal of Operational Research 294 (2021) 723–733. doi:10.1016/j.ejor.2021.02.008.

[74] L. Gurobi Optimization, Gurobi Optimizer Reference Manual, 2023. URL: https://www.gurobi.com.

[75] Julia, The Julia Programming Language, 2023. URL: https://julialang.org/.

[76] S. Herrera-León, F. A. Lucay, L. A. Cisternas, A. Kraslawski, Applying a multi-objective optimization approach in designing water supply systems for mining industries. The case of Chile, Journal of Cleaner Production 210 (2019). doi:10.1016/j.jclepro.2018.11.081.

[77] Iberdrola, Power Purchase Agreements, 2024. URL: https://www.iberdrola.com/about-us/contracts-ppa-energy.

[78] Y. Ghiassi-Farrokhfal, W. Ketter, J. Collins, Making green power purchase agreements more predictable and reliable for companies, Decision Support Systems 144 (2021) 113514. URL: https://doi.org/10.1016/j.dss.2021.113514. doi:10.1016/j.dss.2021.113514.

[79] L. Mendicino, D. Menniti, A. Pinnarelli, N. Sorrentino, Corporate power purchase agreement: Formulation of the related levelized cost of energy and its application to a real life case study, Applied Energy 253 (2019) 113577. URL: https://doi.org/10.1016/j.apenergy.2019.113577. doi:10.1016/j.apenergy.2019.113577.

[80] CNE, Tarificación, 2024. URL: https://www.cne.cl/tarificacion/electrica/.

[81] Coordinador Eléctrico Nacional, Sistema Eléctrico Nacional, 2024. URL: https://www.coordinador.cl/sistema-electrico/#:~:text=Porlascaractersticasdela,deChilo%2Cenelsur.

[82] W. Spark, El clima y el tiempo promedio en todo el año en Calama, 2024. URL: https://es.weatherspark.com/y/27338/Clima-promedio-en-Calama-Chile-durante-todo-el-ao#Figures-Temperature.